glycine. Filters were transferred into lysis buffer (1% TX-100, 20 mM HEPES, 1 mM EDTA, 100 mM NaCl, aprotinin 10 μg/ml, leupeptin 10 μg/ml, and phenylmethylsulfonylfluoride 250 μM) for 30 min on ice and vortexed, and solubilized material was cleared by centrifugation at 14,000 rpm at 4 C for 15 min. An aliquot of cleared supernatant served as the total expression sample, and the remainder was incubated with streptavidin-agarose (Sigma Chemical Co., St. Louis, MO) to recover biotinylated proteins. Immunoprecipitated proteins were subjected to SDS-PAGE and subsequent Western blot analysis using either a polyclonal LDL-R antibody, LB1 (gift from Dr. P. Kroon, Department of Biochemistry, University of Queensland), or antibodies specific to hGLUT1 (gift from Dr. G. Lienhard, Department of Biochemistry, Dartmouth Medical School, Hanover, NH). Detection was performed using goat antirabbit-horseradish peroxidase antibody (Amersham Life Science) and enhanced chemiluminescence (SuperSignal, Pierce Chemical Co.).

Acknowledgments

Received March 18, 2003. Accepted October 30, 2003.

Address all correspondence and requests for reprints to: David E. James, Garvan Institute of Medical Research, St. Vincents Hospital, Sydney 2010, Australia. E-mail: d.james@garvan.org.au; or Yoshitomo Oka, Division of Molecular Metabolism and Diabetes, Department of Internal Medicine Tohoku University Graduate School of Medicine, Miyagi 980-8574, Japan. E-mail: oka@int3.med.tohoku.ac.jp.

K.I. and A.M.S. contributed equally to this work and should both be considered first authors.

This work was supported by the Research Council of Australia, of which D.E.J. is a Senior Principal Research Fellow of the National Health and Medical Research Council of Australia. This work was also supported by Grant-in Aid for Scientific Research no. 13470226 (to Y.O.) and Creative Basic Research Grant no. 10NP0201 (to Y.O.) from the Ministry of Education, Culture, Sports, Science, and Technology of Japan.

REFERENCES

1. Matter K, Mellman I 1994 Mechanisms of cell polarity: sorting and transport in epithelial cells. Curr Opin Cell Biol 6:545–554
2. Simon K, Wandinger-Ness A 1990 Polarized sorting in epithelia. Cell 62:207–210
3. Casanova JE, Apodaca G, Mostov KE 1991 An autonomous signal for basolateral sorting in the cytoplasmic domain of the polymeric immunoglobulin receptor. Cell 66:65–75
4. Hunziker W, Harter C, Matter K, Mellman I 1991 Basolateral sorting in MDCK cells requires a distinct cytoplasmic domain determinant. Cell 66:907–920
5. Marks MS, OhnoH, Kirchhausen T, Bonifacino JS 1997 Protein sorting by tyrosine-based signals: adapting to the Ys and wherefores. Trends Cell Biol 7:124–128
6. Pond L, Kuhn LA, Teyton L, Schutze MP, Tainer JA, Jackson MR, Peterson PA 1995 A role for acidic residues in di-leucine motif-based targeting to the endocytic pathway. J Biol Chem 270:19989–19997
7. Sandoval IV, Bakke O 1994 Targeting of membrane proteins to endosomes and lysosomes. Trends Cell Biol 4:292–297
8. Rapoport I, Chen YC, Cupers P, Shoelson S, Kirchhausen T 1998 Dileucine-based sorting signals bind to the β chain of AP-1 at a site distinct and regulated differently from the tyrosine-based motif-binding site. EMBO J 17:2148–2155
9. Rapoport I, Moyazaki M, Boll W, Duckworth B, Cantley LC, Shoelson S, Kirchhausen T 1997 Regulatory interactions in the recognition of tyrosine-based endocytic signals by clathrin AP-2 complexes. EMBO J 16:2240–2250
10. Rodionov DG, Bakke O 1998 Medium chains of adaptor complexes AP-1 and AP-2 recognize leucine-based sorting signals from the invariant chain. J Biol Chem 273: 6005–6008
11. Urban J, Parczyk K, Leutz A, Kayne M, Kondor-Koch C 1987 Constitutive apical secretion of an 80-kD sulfated glycoprotein complex in the polarized epithelial Madin-Darby canine kidney cell line. J Cell Biol 105:2735–2743
12. Kitagawa Y, Sano Y, Ueda M, Higashio K, Narita H, Okano M, Matsumoto S, Sasaki R 1994 N-glycosylation of erythropoietin is critical for apical secretion by Madin-Darby canine kidney cells. Exp Cell Res 213:449–457
13. Jacob R, Alfalah M, Grunberg J, Obendorf M, Naim HY 2000 Structural determinants required for apical sorting of an intestinal brush-border membrane protein. J Biol Chem 275:6566–6572
14. Monlauzeur L, Breuza L, Le Bivic A 1998 Putative O-glycosylation sites and a membrane anchor are necessary for apical delivery of the human neurotrophin receptor in Caco-2 cells. J Biol Chem 273:30263–30270
15. Bell GI, Kayano T, Buse JB, Burant CF, Takeda J, Lin D, Fukumoto H, Seino S 1990 Molecular biology of mammalian glucose transporter. Diabetes Care 13:198–208
16. Thorens B, Cheng ZQ, Brown D, Lodish HF 1990 Liver glucose transporter: a basolateral protein in hepatocytes and intestine and kidney cells. Am J Physiol 259: C279–C285
17. Rand EB, Depaoli AM, Davidson NO, Bell GI, Burant CF 1993 Sequence, tissue distribution, and functional characterization of the rat fructose transporter GLUT5. Am J Physiol 264:G1169–G1176
18. Harris DS, Slot JW, Geuze HJ, James DE 1992 Polarized distribution of glucose transporter isoforms in Caco-2 cells. Proc Natl Acad Sci USA 89:7556–7560
19. Davidson NO, Hausman AML, Ifkovits CA, Buse JB, Gould GW, Burant CF, Bell GI 1992 Human intestinal glucose transporter expression and localization of GLUT5. Am J Physiol 262:C795–C800
20. Pascoe WS, Inukai K, Oka Y, Slot JW, James DE 1996 Differential targeting of facilitative glucose transporter in polarized epithelial cells. Am J Physiol 271:C547–C554
21. Inukai K, Katagiri H, Takata K, Asano T, Anai M, Ishihara H, Nakazaki M, Kikuchi M, Yazaki Y, Oka Y 1995 Characterization of rat GLUT5 and functional analysis of chimeric proteins of GLUT1 glucose transporter and GLUT5 fructose transporter. Endocrinology 136:4850–4857
22. Colville CA, Seatter MJ, Jess TJ, Gould GW, Thomas HM 1993 Kinetic analysis of the liver-type (GLUT2) and brain-type (GLUT3) glucose transporter in *Xenopus* oocytes: substrates specificities and effects of transport inhibitors. Biochem J 290:701–706
23. Davies A, Ciardelli TL, Lienhard GE, Boyle JM, Whetton AD, Baldwin SA 1990 Site-specific antibodies as probes of the topology and function of the human erythrocyte glucose transporter. Biochem J 266:799–808
24. Matter K, Hunziker W, Mellman I 1992 The cytoplasmic domain contains two tyrosine-dependent targeting determinants. Cell 71:741–753
25. Matter K, Whitney JA, Yamamoto EM, Mellman I 1993 Common signals control low density lipoprotein receptor sorting in endosomes and the Golgi complex of MDCK cells. Cell 74:1053–1064
26. Inukai K, Takata K, Asano T, Katagiri H, Ishihara H, Nakazaki M, Fukushima Y, Yazaki Y, Kikuchi M, Oka Y 1997 Targeting of GLUT1-GLUT5 chimeric proteins in the polarized cell line Caco-2. Mol Endocrinol 11:442–449
27. Shewan AM, Marsh BJ, Melvin DR, Martin S, Gould GW, James DE 2000 The cytosolic C-terminus of the glucose transporter GLUT4 contains an acidic cluster endosomal

targeting motif distal to the dileucine signal. Biochem J 350:99–107
28. Piper RC, Tai C, Kulesza P, Pang S, Warnock D, Baenziger J, Slot JW, Geuze HJ, Puri C, James DE 1993 GLUT4 NH2 terminus contains a phenylalanine-based targeting motif that regulates intracellular sequestration. J Cell Biol 121:1221–1232
29. Bunn RC, Jensen MA, Reed BC 1999 Protein interactions with the glucose transporter binding protein GLUT1CBP that provide a link between GLUT1 and the cytoskeleton. Mol Biol Cell 10:819–832
30. Songyang Z, Fanning AS, Fu C, Xu J, Marfatia SM, Chishti AH, Crompton A, Chan AC, Anderson JM, Cantley LC 1997 Recognition of unique carboxy-terminal motifs by distinct PDZ domains. Science 275:73–77
31. Brown D, Rose J 1991 Sorting of GPI-anchored protein to glycolipid-enriched membrane subdomains during transport to the apical cell surface. Cell 68:533–544
32. Sakyo T, Kitagawa T 2002 Differential localization of glucose transporter isoforms in non-polarized mammalian cells: distribution of GLUT1 but not GLUT3 to detergent-resistant membrane domains. Biochim Biophys Acta 1567:165–175
33. Jolimay N, Franck L, Langlois X, Hamon M, Darmon M 2000 Dominant role of the cytosolic C-terminal domain of the rat 5-HT1B receptor in axonal-apical targeting. J Neurosci 20:9111–9118
34. Tugizov S, Maidji E, Xiao J, Zheng Z, Pereira L 1998 Human cytomegalovirus glycoprotein B contains autonomous determinants for vectorial targeting to apical membranes of polarized epithelial cells. J Virol 72: 7374–7386
35. Milewski MI, Mickle, JE, Forrest JK, Stafford DM, Moyer BD, Cheng J, Guggino WB, Stanton BA, Cutting GR 2001 A PDZ-binding motif is essential but not sufficient to localize the C terminus of CFTR to the apical membrane. J Cell Sci 114:719–726
36. Sun AQ, Salkar R, Xu SS, Zeng L, Zhou MM, Suchy FJ 2003 A 14-amino acid sequence with a β-turn structure is required for apical membrane sorting of the rat ileal bile acid transporter. J Biol Chem 278:4000–4009
37. Chuang JZ, Sung CH 1998 The cytoplasmic tail of rhodopsin acts as a novel apical sorting signal in polarized MDCK cells. J Cell Biol 142:1245–1256
38. Heijnen HF, Oorschot V, Sixma JJ, Slot JW, James DE 1997 Thrombin stimulates glucose transport in human platelet via translocation of the glucose transporter GLUT3 from α-granules to the cell surface. J Cell Biol 138:323–330
39. Angulo C, Rauch MC, Droppelmann A, Reyers AM, Slebe JC, Delgado-Lopez F, Guaiquil VH, Vera JC, Concha II 1998 Hexose transporter expression and function in mammalian spermatozoa: cellular localization and transport of hexoses and vitamin C. J Cell Biochem 71: 189–203
40. Thoidis G, Kupriyanova T, Cunningham JM, Chen P, Cadel S, Foulon T, Cohen P, Fine RE, Kandror KV 1999 Glucose transporter GLUT3 is targeted to secretory vesicles in neurons and PC12 cells. J Biol Chem 274: 14062–14066
41. Dotti CG, Simons K 1990 Polarized sorting of viral glycoproteins to the axon and dendrites of hippocampal neurons in culture. Cell 62:63–72
42. Katagiri H, Asano T, Ishihara H, Tsukuda K, Lin JL, Inukai K, Kikuchi M, Yazaki Y, Oka Y 1992 Replacement of intracellular C-terminal domain of GLUT1 glucose transporter with that of GLUT2 increases V_{max} and K_m of transport activity. J Biol Chem 267:22550–22555
43. Inukai K, Asano T, Katagiri H, Ishihara H, Anai M, Fukushima Y, Tsukuda K, Kikuchi M, Yazaki Y, Oka Y 1993 Cloning and increased expression with fructose feeding of rat jejunal GLUT5. Endocrinology 133: 2009–2014

Molecular Endocrinology **is published monthly by The Endocrine Society (http://www.endo-society.org), the foremost professional society serving the endocrine community.**

Am J Physiol Endocrinol Metab 286: E280–E285, 2004.
First published October 7, 2003; 10.1152/ajpendo.00380.2003.

Overexpression of constitutively activated glutamate dehydrogenase induces insulin secretion through enhanced glutamate oxidation

Takatoshi Anno,[1] Shunsuke Uehara,[2] Hideki Katagiri,[3] Yasuharu Ohta,[1] Kohei Ueda,[1] Hiroyuki Mizuguchi,[4] Yoshinori Moriyama,[2] Yoshitomo Oka,[3] and Yukio Tanizawa[1]

[1]*Division of Molecular Analysis of Human Disorders, Department of Bio-Signal Analysis, Yamaguchi University Graduate School of Medicine, Ube, Yamaguchi 755-8505;* [2]*Department of Biochemistry, Faculty of Pharmaceutical Sciences, Okayama University, Okayama 700-8530;* [3]*Division of Molecular Metabolism and Diabetes, Department of Internal Medicine, Tohoku University Graduate School of Medicine, Sendai 980-8574; and* [4]*Division of Cellular and Gene Therapy Products, National Institute of Health Sciences, Tokyo 158-8501, Japan*

Submitted 25 August 2003; accepted in final form 2 October 2003

Anno, Takatoshi, Shunsuke Uehara, Hideki Katagiri, Yasuharu Ohta, Kohei Ueda, Hiroyuki Mizuguchi, Yoshinori Moriyama, Yoshitomo Oka, and Yukio Tanizawa. Overexpression of constitutively activated glutamate dehydrogenase induces insulin secretion through enhanced glutamate oxidation. *Am J Physiol Endocrinol Metab* 286: E280–E285, 2004. First published October 7, 2003; 10.1152/ajpendo.00380.2003.—Glutamate dehydrogenase (GDH) catalyzes reversible oxidative deamination of L-glutamate to α-ketoglutarate. Enzyme activity is regulated by several allosteric effectors. Recognition of a new form of hyperinsulinemic hypoglycemia, hyperinsulinism/hyperammonemia (HI/HA) syndrome, which is caused by gain-of-function mutations in GDH, highlighted the importance of GDH in glucose homeostasis. GDH266C is a constitutively activated mutant enzyme we identified in a patient with HI/HA syndrome. By overexpressing GDH266C in MIN6 mouse insulinoma cells, we previously demonstrated unregulated elevation of GDH activity to render the cells responsive to glutamine in insulin secretion. Interestingly, at low glucose concentrations, basal insulin secretion was exaggerated in such cells. Herein, to clarify the role of GDH in the regulation of insulin secretion, we studied cellular glutamate metabolism using MIN6 cells overexpressing GDH266C (MIN6-GDH266C). Glutamine-stimulated insulin secretion was associated with increased glutamine oxidation and decreased intracellular glutamate content. Similarly, at 5 mmol/l glucose without glutamine, glutamine oxidation also increased, and glutamate content decreased with exaggerated insulin secretion. Glucose oxidation was not altered. Insulin secretion profiles from GDH266C-overexpressing isolated rat pancreatic islets were similar to those from MIN6-GDH266C, suggesting observation in MIN6 cells to be relevant in native β-cells. These results demonstrate that, upon activation, GDH oxidizes glutamate to α-ketoglutarate, thereby stimulating insulin secretion by providing the TCA cycle with a substrate. No evidence was obtained supporting the hypothesis that activated GDH produced glutamate, a recently proposed second messenger of insulin secretion, by the reverse reaction, to stimulate insulin secretion.

hypoglycemia; hyperinsulinism/hyperammonemia syndrome; islet of Langerhans

THE MITOCHONDRIAL MATRIX ENZYME glutamate dehydrogenase (GDH; EC 1.4.1.3) catalyzes reversible oxidative deamination of L-glutamate to α-ketoglutarate with NAD(P) as a cofactor. The activity of this enzyme is regulated positively and negatively by several allosteric effectors, including amino acids (leucine, isoleucine, valine, methionine), ADP, and GTP. In pancreatic β-cells, GDH has been suggested to be involved in the regulation of insulin secretion, especially leucine-stimulated insulin secretion (18, 19). The importance of GDH in glucose homeostasis is also evident from recent findings that gain-of-function mutations in the GLUD1 gene, which encodes GDH, cause hyperinsulinism /hyperammonemia (HI/HA) syndrome (9, 20, 21, 22, 25, 29).

Previously, we identified a GLUD1 gene mutation, Y266C, in a patient with HI/HA syndrome (22). The activity of the mutant GDH (GDH266C) was constitutively elevated, and allosteric regulations by ADP and GTP were severely impaired. Using GDH266C as a tool, we showed unregulated elevation of GDH activity in MIN6 insulinoma cells to render the cells responsive to glutamine. Glutamine stimulated insulin secretion from these cells in the absence of leucine, an allosteric activator of GDH. We also demonstrated insulin secretion to be exaggerated in these cells at low glucose concentrations (22). Glutamine alone, to which the plasma membrane is permeable and which is readily converted to glutamate intracellularly, does not normally stimulate insulin release. However, it remarkably stimulates insulin secretion in the presence of leucine. It is generally accepted that, in pancreatic β-cells, activation of GDH by allosteric effectors, such as leucine, enhances glutamate oxidation and increases ATP production by providing the tricarboxylic acid (TCA) cycle with α-ketoglutarate and thereby stimulates insulin secretion (18, 19). Physiologically, GDH is also suggested to play an important role in basal insulin secretion (2, 5). Our previous observations (22) in MIN6 cells are in good agreement with this theory.

On the other hand, mitochondrially derived glutamate was suggested to be a second messenger in glucose-stimulated insulin secretion, acting directly on insulin-secretory granules (4, 11, 17). This theory assumes reverse flux through GDH in the direction of glutamate formation, and glutamate-induced insulin secretion was suggested to correlate with the level of GDH expression (4, 10). However, this hypothesis is controversial and has been contradicted by other studies (2, 8). Furthermore, it was recently demonstrated that cellular glutamate content did not correlate with the amplification of insulin secretion (1, 7). Most previous studies have investigated the role of GDH in insulin secretion by activating intracellular

Address for reprint requests and other correspondence: Y. Tanizawa, Div. of Molecular Analysis of Human Disorders, Dept. of Bio-Signal Analysis, Yamaguchi Univ. Graduate School of Medicine, Minami-Kogushi Ube, Yamaguchi 755-8505, Japan (E-mail: tanizawa@yamaguchi-u.ac.jp).

The costs of publication of this article were defrayed in part by the payment of page charges. The article must therefore be hereby marked "*advertisement*" in accordance with 18 U.S.C. Section 1734 solely to indicate this fact.

GDH with allosteric activators such as leucine or β-2-aminobicyclo[2.2.1]heptane-2-carboxylic acid. Identification of constitutively activated mutant GDH (GHD266C) enabled us to study the effects of elevated intracellular GDH activity on insulin secretion more directly by introducing the mutant enzyme into cells. Our present study was designed to investigate directly the correlations among insulin secretion, GDH activity, and cellular glutamate metabolism. We also studied changes in insulin secretion profiles caused by unregulated elevation of GDH activity in native β-cells to confirm the physiological relevance of our findings in MIN6 cells. Our results further clarify the role of GDH in the regulation of insulin secretion and provide insights into the pathophysiology of the HI/HA syndrome.

MATERIALS AND METHODS

Analysis of glutamine and glucose oxidation. MIN6 cells overexpressing the mutant GDH via retrovirus-mediated gene transfer (MIN6-GDH266C) and control lacZ-overexpressing cells (MIN6-lacZ) were used for these experiments (22). Cells were seeded onto a 6-cm dish at a concentration of 4.0×10^6 cells/dish and cultured in DMEM-MIN6 medium (Sigma, St. Louis, MO) containing 25 mmol/l glucose supplemented with 15% heat-inactivated fetal calf serum, 72 μmol/l β-mercaptoethanol, 50 U/ml penicillin G, and 50 μg/ml streptomycin. Sixty hours later, glutamine or glucose oxidation was assayed. After a 30-min preincubation in HEPES-balanced Krebs-Ringer bicarbonate buffer (HB-KRBB; in mmol/l: 10 HEPES, 120 NaCl, 4.7 KCl, 1.2 $MgSO_4$, 1.2 KH_2PO_4, 20 $NaHCO_3$, and 2 $CaCl_2$, pH 7.4) containing 0.5% BSA and 5 mmol/l glucose, radioactive L-[U-^{14}C]glutamine (0.05 μCi, 261 Ci/mol; Amersham, Buckinghamshire, UK) or radioactive D-[6-^{14}C]glucose [0.04 μCi (for 5 mmol/l glucose) or 0.20 μCi (for 25 mmol/l glucose), 58.0 Ci/mol; Amersham] was added to 4 ml of fresh HB-KRBB containing 0.5% BSA and various concentrations of glutamine or glucose. Then, MIN6-GDH266C or MIN6-lacZ cells in the culture dishes were placed immediately in sealed glass containers (7 cm diameter × 10 cm height) filled with 100% oxygen and incubated for 30 min (glutamine oxidation) or 1 h (glucose oxidation) at 37°C. At completion of the incubations, 0.5 ml of 10% $HClO_4$ was added to the medium by means of a long 21-gauge needle through rubber stoppers on the top of the container, allowing CO_2 gas (containing radioactive [^{14}C]CO_2) to evaporate and be trapped in 2 ml of 10% KOH solution in a small glass cup suspended above the medium in a sealed glass container. The glass containers were incubated for another 30 min, and the KOH solution was then transferred to scintillation vials containing 10 ml of Aquasol-2 (PerkinElmer, Boston, MA), and radioactivity was measured with a liquid scintillation counter. With this system, 90.7 ± 1.2% (mean ± SE; $n = 3$) of CO_2 gas, evaporating from the medium containing 0.5 μCi NaH[^{14}C]O_3 (Amersham), was trapped in KOH solution.

Measurement of intracellular glutamate content. MIN6-GDH266C and control MIN6-lacZ cells were seeded onto six-well plates at a concentration of 1.8×10^6 cells/well and cultured in DMEM-MIN6 medium. Sixty hours later, glutamate contents were assayed. After a 30-min preincubation in HB-KRBB containing 0.5% BSA and 5 mmol/l glucose, the preincubation buffer was replaced with fresh HB-KRBB containing 0.5% BSA and various concentrations of glutamine or glucose, and the cells were incubated for an additional hour at 37°C. At the end of the incubation, the cells were quickly washed on ice with ice-cold HB-KRBB, and 1 ml of 6% perchloric acid was immediately added. The cells were then collected and sonicated on ice. After centrifugation at 15,000 rpm for 5 min, the supernatant (800 μl) was collected, and 275 μl of 30% KOH were added. White precipitates were removed by brief centrifugation, and the supernatant was kept at −80°C for the glutamate measurement. Cells in one of the wells were homogenized in PBS and used for protein determination. The amount of glutamate was determined, using an aliquot of the cell extract, by high-performance liquid chromatography with precolumn *o*-phthalaldehyde derivatization, separation on a reverse-phase Resolve C18 column (3.9 × 150 mm; Waters, Toronto, ON, Canada), and fluorescence detection (3, 27, 28).

Construction of recombinant adenoviruses and adenovirus-mediated gene transfer. pcDNA3-hGDH-WT and pcDNA3-hGDH266C (22) were digested with *Not*I and *Sna*BI. The fragments containing GDH cDNA were then ligated into *Not*I- and *Sna*BI-digested pShuttle vectors (14, 15). The resultant plasmids, pShuttle-hGDH-WT and pShuttle-hGDH266C, were then digested with I-*Ceu*I/PI-*Sce*I and ligated into I-*Ceu*I/PI-*Sce*I-digested pAdHM4 (14, 15) to produce pAd-hGDH-WT and pAd-hGDH266C. They were then linearized with *Pac*I and transfected into 293 human embryonic kidney cells with FuGENE6 (Roche Diagnostics, Mannheim, Germany) according to the manufacturer's instructions. Recombinant adenoviruses expressing GDH-WT and GDH266C (Ad-hGDH-WT and Ad-hGDH266C) were thus obtained and amplified via infection of 293 cells. As a control, we also constructed an adenoviral vector to express enhanced green fluorescent protein (eGFP; Ad-eGFP). Titers of the recombinant adenovirus stocks were 6.0×10^7 (Ad-hGDH-WT), 5.5×10^7 (Ad-hGDH266C), and 9.5×10^7 plaque-forming units (pfu)/ml (Ad-eGFP).

Pancreatic islets were isolated by collagenase digestion as described previously (6, 24). Isolated islets were cultured on a 60-mm tissue culture dish with RPMI 1640 medium containing 11 mmol/l glucose supplemented with 10% fetal calf serum, 50 U/ml penicillin, and 50 μg/ml streptomycin (RPMI-islet) and maintained at 37°C in humidified 5% CO_2-95% air. Twenty-four to thirty-six hours after isolation, groups of 50–100 islets were incubated with the recombinant adenoviruses at a multiplicity of infection (moi) of $\sim 4 \times 10^5$ pfu/islet. After a 1-h incubation with the adenovirus at 37°C, the medium was removed, and the islets were washed once with phosphate-buffered saline (PBS). The islets were then further incubated on a 60-mm tissue culture dish with RPMI-islet medium. Experiments were performed 24 h after infection.

GDH enzyme assay. COS-7 cells and isolated pancreatic islets were infected with recombinant adenoviruses at an moi of ~10 pfu/cell or 4×10^5 pfu/islet, respectively. Forty-eight (COS-7) or 24 (islets) h after the infection, cells were washed, suspended in PBS, and sonicated to prepare crude cell extract. GDH activity was measured by the oxidation of NADH ($\epsilon_{340\ nm} = 6.22 \times 10^3$ mol·l^{-1}·cm^{-1}), as described previously (26), with a Beckman Coulter (Fullerton, CA) Spectrophotometer model DU-640 at 25°C. The assay solution (1 ml) consisted of 10 mmol/l Tris-acetate (pH 8.0), 10 μmol/l EDTA, 100 μmol/l NADH, 50 mmol/l NH_4Cl, and 5 mmol/l α-ketoglutarate. ADP, GTP, or leucine was added to the solution at various concentrations. The reaction was started by adding appropriate amounts (30–50 μl) of cell extracts, and the decrease in absorbance at 340 nm was measured for 5 min. During this incubation period, the reaction was linear, and there was no indication of GTP hydrolysis, substrate depletion, or product saturation. The activity was determined in duplicate for each sample.

Analysis of insulin secretion. Groups of 10–30 islets overexpressing the mutant GDH (Islets-GDH266C) and eGFP (Islets-eGFP) via adenovirus-mediated gene transfer were used for each assay. Insulin secretion was examined by the static incubation method (23, 24). In brief, after a 30-min preincubation in HB-KRBB supplemented with 0.5% BSA and 5 mmol/l glucose, the preincubation buffer was replaced with fresh HB-KRBB containing 0.5% BSA and various concentrations of glutamine or glucose. After an additional 30-min incubation at 37°C, the buffer was collected, and immunoreactive insulin was measured by radioimmunoassay using rat insulin (Linco Research, St. Charles, MO) as a standard. The amounts of secreted insulin were corrected by the amounts of cell protein in each well.

RESULTS

Glutamine and glucose metabolism in MIN6-GDH266C cells. We investigated the metabolic changes associated with elevated GDH activity. We used MIN6-GDH266C as a model. When the cells were incubated in the presence of glutamine (1 mmol/l) with a tracer of L-[U-^{14}C]glutamine, glutamine oxidation was increased in MIN6-GDH266C compared with control MIN6-lacZ ($P < 0.02$, unpaired *t*-test; Fig. 1*A*). In agreement with the enhanced glutamine oxidation, intracellular glutamate content in MIN6-GDH266C was lower than that in MIN6-lacZ ($P < 0.01$ at 1.0 mmol/l; Fig. 1*B*).

At low glucose concentrations (without exogenous glutamine), insulin secretion was augmented in MIN6-GDH266C (22). We then studied metabolic changes under these conditions. Glucose oxidation did not differ between MIN6-GDH266C and MIN6-lacZ [4.0 ± 0.7 vs. 4.0 ± 0.9 pmol/μg protein at 5 mmol/l glucose ($P > 0.9$; Fig. 2*A*) and 7.9 ± 2.0 vs. 6.8 ± 1.9 pmol/μg protein at 25 mmol/l glucose ($P > 0.6$; unpaired *t*-test)]. Cellular glutamine oxidation, however, was significantly enhanced in MIN6-GDH266C [46.7 ± 1.2 vs. 27.2 ± 1.6 pmol/μg protein at 5 mmol/l glucose ($P < 0.001$; Fig. 2*B*) and 31.7 ± 4.1 vs. 16.4 ± 2.0 pmol/μg protein at 25 mmol/l glucose ($P < 0.03$; unpaired *t*-test)]. The corresponding intracellular glutamate content was decreased in MIN6-GDH266C compared with that in MIN6-lacZ [10.3 ± 2.0 vs. 25.4 ± 2.3 pmol/μg protein at 5 mmol/l glucose ($P < 0.002$; Fig. 2*C*) and 14.2 ± 1.3 vs. 36.6 ± 2.1 pmol/μg protein at 25 mmol/l glucose ($P < 0.001$; unpaired *t*-test)]. These results indicate that elevated GDH activity enhances glutamine oxidation and probably increases ATP synthesis via the TCA cycle, thereby stimulating insulin secretion.

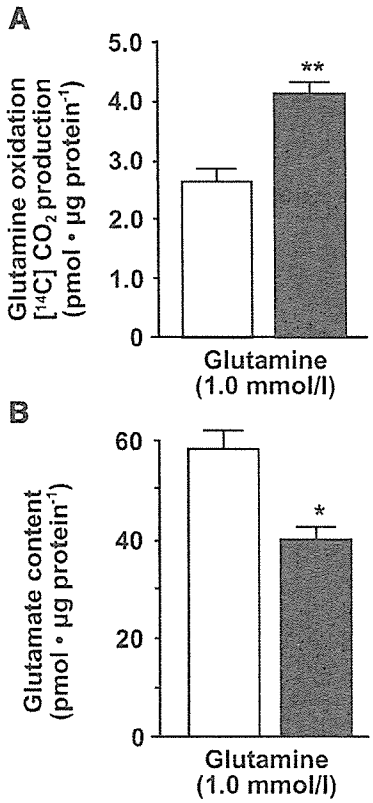

Fig. 1. Glutamine oxidation and glutamate content in MIN6 cells incubated in the presence of glutamine. *A*: glutamine oxidation. MIN6 cells overexpressing consitutively activated mutant glutamate dehydrogenase (GDH; MIN6-GDH266C; filled bar) and MIN6 cells overexpressing lacZ (MIN6-lacZ; open bar) were preincubated in HEPES-balanced Krebs-Ringer bicarbonate buffer (HB-KRBB) with 5 mmol/l glucose for 30 min at 37°C, followed by incubation in HB-KRBB with 1 mmol/l L-[U-^{14}C]glutamine for 30 min at 37°C. [^{14}C]CO_2 produced by the MIN6 cells was trapped in KOH solution and radioactivity determined by liquid scintillation counting. Data are means ± SE of 3 experiments. $^{**}P < 0.02$ for comparison between MIN6-GDH266C and MIN6-lacZ (unpaired Student's *t*-test). *B*: glutamate contents. MIN6-GDH266C (filled bar) and MIN6-lacZ (open bar) cells were preincubated at 37°C in HB-KRBB with 5 mmol/l glucose for 30 min, followed by incubation at 37°C in the presence of 1 mmol/l glutamine for 1 h. Immediately after incubation, cells were quickly homogenized in ice-cold perchloric acid solution. The solution was neutralized and the supernatant saved at −80°C for the glutamate assay. Glutamate content was determined by HPLC. Data are means ± SE of 5 experiments. $^{*}P < 0.01$ for comparison between MIN6-GDH266C and MIN6-lacZ (unpaired Student's *t*-test).

Characterizations of GDH266C expressed in COS-7 cells and in isolated rat pancreatic islets. To overexpress GDH266C in isolated rat pancreatic islets, we constructed a recombinant adenovirus, Ad-hGDH266C. As we previously demonstrated using the enzyme expressed in COS-7 cells (22), basal activity (activity in the absence of allosteric effecters) of GDH266C was elevated, and inhibition by GTP and activation by ADP were blunted compared with those of the wild-type enzyme. Here, we further characterized activation by leucine by using COS-7 cell extracts in which wild-type GDH or GHD266C was overexpressed by adenovirus-mediated gene transduction. Activation of GDH266C by leucine was only twofold (from 2,850 ± 120 to 5,520 ± 190 nmol NADH·mg protein^{-1}·min^{-1} at 3 mmol/l leucine), whereas that of wild-type GDH was more than 35-fold (from 130 ± 20 to 4,670 ± 70 nmol NADH·mg protein^{-1}·min^{-1} at 3 mmol/l leucine). Maximal activity of GDH266C in the presence of leucine was nearly the same as that of the wild-type enzyme in the crude cell extracts, although analysis of the purified enzyme was necessary for the strict quantitative comparison.

Next, we overexpressed GDH266C in isolated islets (Islets-GDH266C) using the adenovirus-mediated gene transfer system to investigate the role of GDH in native β-cells. Islets overexpressing eGFP (Islets-eGFP) were used as a control. Transfer of exogeneous genes with adenovirus vector to islets was very efficient, and most of the islet cells expressed eGFP when they were infected with Ad-eGFP, as confirmed by observation under fluorescence microscopy (Ref. 24 and data not shown). The basal GDH activities in the crude extracts of Islets-eGFP and Islets-GDH266C were 20 ± 3 and 2,890 ± 670 nmol NADH·mg protein^{-1}·min^{-1}, respectively, when activity was measured without allosteric effectors in the reaction mixture (Table 1). As expected, ADP activated GDH activity 20-fold in the crude extract of Islets-eGFP (510 ± 50 nmol NADH·mg protein^{-1}·min^{-1} at 200 μmol/l ADP), whereas activation in the extract of Islets-GDH266C was less than twofold (4,570 ± 650 nmol NADH·mg protein^{-1}·min^{-1} at 200 μmol/l ADP). GTP did not inhibit GDH activity in Islets-GDH266C (2,840 ± 600 nmol NADH·mg protein^{-1}·min^{-1} at 25 μmol/l GTP). Therefore, in Islets-GDH266C, GDH activity was constitutively elevated.

Profiles of insulin secretion from Islets-GDH266C. It is known that in normal pancreatic β-cells glutamine stimulates

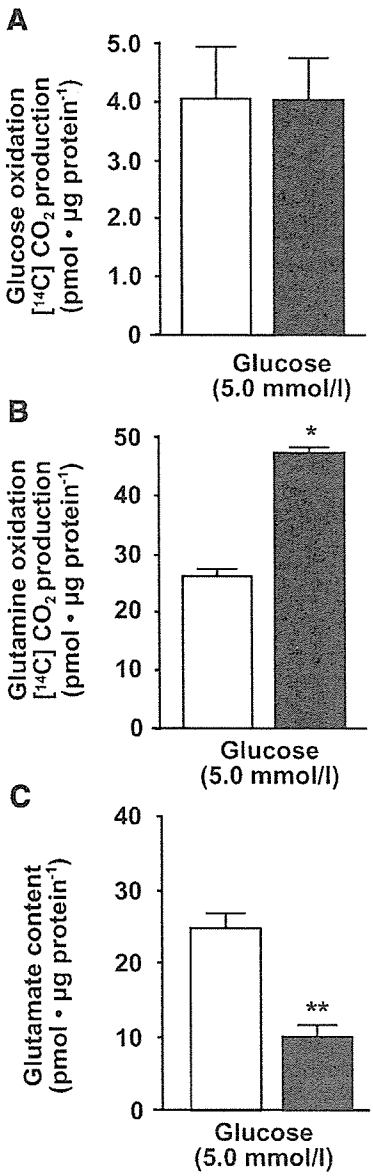

Fig. 2. Glutamine oxidation and glutamate content in MIN6 cells incubated in the presence of 5 mmol/l glucose. *A*: glucose oxidation. MIN6-GDH266C (filled bar) and MIN6-lacZ (open bar) cells were preincubated in HB-KRBB with 5 mmol/l glucose for 30 min at 37°C, followed by incubation in HB-KRBB with 5 mmol/l D-[6-^{14}C]glucose for 1 h at 37°C. [^{14}C]CO_2 produced by the MIN6 cells was trapped in KOH solution and radioactivity determined by liquid scintillation counting. Data are means ± SE of 6 experiments. *B*: glutamine oxidation. MIN6-GDH266C (filled bar) and MIN6-lacZ (open bar) cells were preincubated at 37°C in HB-KRBB with 5 mmol/l glucose for 30 min, followed by incubation at 37°C for 30 min in the presence of 5 mmol/l glucose and a tracer of radioactive L-[U-^{14}C]glutamine. Radioactive [^{14}C]CO_2 produced by the MIN6 cells was trapped in KOH solution and radioactivity determined by liquid scintillation counting. Data are means ± SE of 3 experiments. *$P < 0.001$ for comparison between MIN6-GDH266C and MIN6-lacZ (unpaired Student's *t*-test). *C*: glutamate contents. MIN6-GDH266C (filled bar) and MIN6-lacZ (open bar) cells were preincubated at 37°C in HB-KRBB with 5 mmol/l glucose for 30 min, followed by incubation at 37°C in the presence of 5 mmol/l glucose for 1 h. After incubation, glutamate contents were measured as described in Fig. 1. Data are means ± SE of 5 experiments. **$P < 0.002$ for comparison between MIN6-GDH266C and MIN6-lacZ (unpaired Student's *t*-test).

Table 1. *GDH activity in Islets-GDH266C and Islets-eGFP*

ADP, µmol/l	GTP, µmol/l	GDH Activity, nmol NADH·mg protein^{-1}·min^{-1} Islets-eGFP	Islets-266C
0	0	20±3	2,890±670
200	0	510±50	4,570±650
0	25	*	2,840±600

Values are means ± SE; $n = 3$. GDH, glutamate dehydrogenase; Islets-GDH266C, islets overexpressing a constitutively activated mutant GDH; Islets-eGFP, islets overexpressing enhanced green fluorescent protein (control). *Below assay sensitivity.

insulin secretion only in the presence of leucine, an allosteric activator of GDH. As shown in Fig. 3*A*, glutamine alone did not stimulate insulin secretion from Islets-eGFP, as was observed with intact islets. On the other hand, it stimulated insulin secretion from Islets-GDH266C in a dose-dependent manner.

Glucose-stimulated insulin secretion was also studied. Insulin secretion from Islets-GDH266C was significantly exaggerated at low glucose concentrations compared with control Islets-eGFP [0.16 ± 0.03 (Islets-eGFP) vs. 0.34 ± 0.09 ng insulin/µg protein (Islets-GDH266C) at 2 mmol/l glucose ($P < 0.05$, $n = 16$); 0.29 ± 0.06 (Islets-eGFP) vs. 0.48 ± 0.07 ng insulin/µg protein (Islets-GDH266C) at 5 mmol/l glucose ($P < 0.001$, $n = 15$); 0.55 ± 0.08 (Islets-eGFP) vs. 0.78 ± 0.15 ng insulin/µg protein (Islets-GDH266C) at 8 mmol/l glucose ($P < 0.05$, $n = 14$); paired *t*-test] but not at higher glucose concentrations (Fig. 3*B*).

DISCUSSION

A mutant GDH, GHD266C, which was identified in a Japanese patient with HI/HA syndrome, is a constitutively activated enzyme: basal activity is elevated, and activation by ADP and inhibition by GTP are blunted compared with the wild-type enzyme (22). In addition, we have herein demonstrated activation by leucine also to be blunted. It has been suggested that ADP binds to and activates GDH by opening the catalytic cleft of the enzyme (16). Leucine is thought to bind at the active site (26). It is possible that in GDH266C the catalytic cleft is almost fully open in the basal state, such that binding of ADP or leucine only minimally activates this mutant enzyme. We used the GDH266C, rather than wild-type GDH, as a tool to examine the effects of elevated cellular GDH activity in the regulation of insulin secretion, because with this mutant, GDH activity is thought to be elevated regardless of phosphate potential (GTP and ATP-to-ADP and P_i ratio) (2, 5) in the cells.

We previously demonstrated glutamine to stimulate insulin secretion from MIN6 cells overexpressing GDH266C (MIN6-GDH266C) in the absence of leucine. In addition, and very interestingly, insulin secretion from MIN6-GDH266C cells was exaggerated at low glucose concentrations (2–5 mmol/l) in the absence of glutamine in the incubation buffer (22). To investigate the mechanism by which elevated cellular GDH activity leads to the stimulation of insulin secretion, we studied changes in glutamate metabolism in cells in which GDH activity was constitutively elevated.

In association with the stimulation of insulin secretion by glutamine, cellular glutamine oxidation was elevated (Fig. 1*A*),

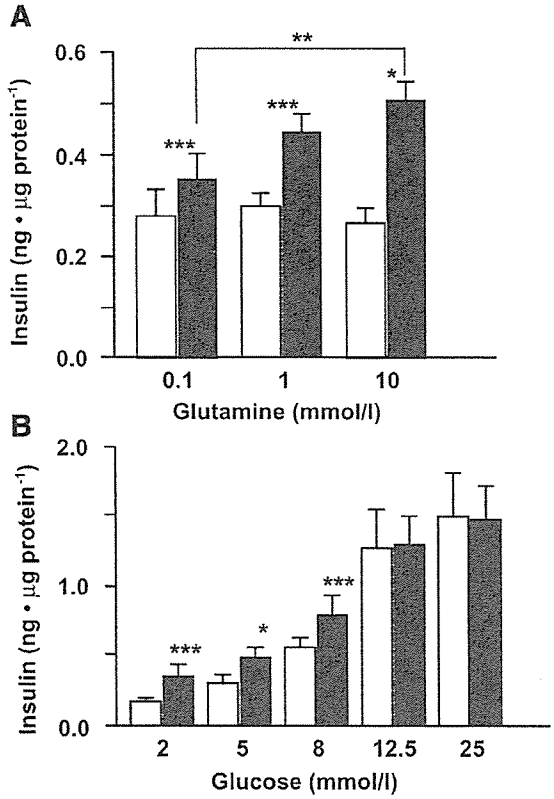

Fig. 3. Glutamine- and glucose-stimulated insulin secretion. *A*: glutamine-stimulated insulin secretion. After a 30-min preincubation in the buffer with 5 mmol/l glucose and without glutamine, pancreatic islets overexpressing GDH266C (Islets-GDH266C; filled bar) and islets overexpressing enhanced green fluorescent protein (Islets-eGFP; open bar) were incubated in the presence of various concentrations of glutamine (without glucose) for 30 min, and insulin released into the incubation buffer was measured. Each assay was performed using 10–30 islets, and values are means ± SE of 3–7 experiments. $*P < 0.01$ and $***P < 0.05$ for comparison between Islets-GDH266C and Islets-eGFP. $**P < 0.02$ for comparison between 0.1 and 10 mmol/l glutamine (Islets-GDH266C) (paired Student's *t*-tests). *B*: glucose-stimulated insulin secretion. After preincubation, Islets-GDH266C (filled bar) and Islets-eGFP (open bar) were incubated in the presence of various concentrations of glucose for 30 min, and insulin released into the incubation buffer was measured. Each assay was performed using 10–30 islets, and values are means ± SE of 6–16 experiments. $*P < 0.01$ and $***P < 0.05$ for comparison between Islets-GDH266C and Islets-eGFP (paired Student's *t*-tests).

and intracellular glutamate content was lower (Fig. 1*B*) in MIN6–266C cells. This observation is consistent with the hypothesis that elevated GDH activity enhances the oxidative deamination of glutamate to α-ketoglutarate to supply TCA cycle substrates (18, 19). It is noteworthy that, at the basal glucose concentration (5 mmol/l) without glutamine in the medium, exaggerated insulin secretion was also associated with enhanced glutamine oxidation, and a decrease in the intracellular glutamate content reflected utilization of the substrate. At this glucose concentration, glutamine (or glutamate) from the intracellular pool would likely be utilized as a substrate of GDH to fuel the TCA cycle and thereby stimulate insulin secretion. At a higher glucose concentration (25 mmol/l), glutamine oxidation also increased, and the cellular glutamate content was lower in MIN6-GDH266C than in MIN6-lacZ cells, although insulin secretion did not differ. Under these conditions, the effect of increased glutamate oxidation on insulin secretion was probably undetectable because glucose stimulation was more potent.

Although the MIN6 cell line is one of the best models of native β-cells (13), it is derived from an insulinoma, and insulin-secretory profiles are known to change over several passages (12). Therefore, this cell line may not adequately reflect native β-cells in some respects. Therefore, we wished to confirm the effect of unregulated elevation of GDH activity on insulin secretion in a more physiological model: isolated rat pancreatic islets. Islets-GDH266C secreted insulin in response to glutamine in a dose-dependent manner (Fig. 3*A*). More importantly, in Islets-GDH266C, insulin secretion was also significantly enhanced at low glucose concentrations (2–8 mmol/l) compared with control Islets-eGFP (Fig. 3*B*), just as we observed in MIN6-GDH266C cells (22). Recently, Kelly et al. (5) reported an H454Y-GDH transgenic mouse. In this animal model, an HI/HA syndrome patient-derived mutant, H454Y-GDH, the activity of which was not inhibited by GTP, was specifically expressed in β-cells. Random blood glucose concentrations were lower than in control mice, and amino acid- and leucine-stimulated insulin secretions from perifused islets were markedly enhanced in these mice. Although glucose-stimulated insulin secretion was reported to be similar to that of control mouse islets, detailed data, including basal insulin secretion at low glucose concentrations, have not been presented. Because basal GDH activity was more than 100 times higher than that in control islets in our model (Table 1), the enhancement of basal insulin secretion might have been more prominent in our model than in the transgenic mouse model.

Physiologically, GDH is an important regulator of glutaminolysis (glutamine oxidation), which may contribute to the interprandial basal insulin secretion (2, 5). Glutaminolysis is regulated by allosteric regulation of GDH with amino acids such as leucine, isoleucine, and methionine. In addition, it is also precisely regulated by glucose metabolism through changes in concentrations of other important allosteric regulators of GDH, GTP, ATP, and ADP. According to this hypothesis, at glucose concentrations near or below its threshold to stimulate insulin secretion (5 mmol/l), GDH is activated by a decrease in the GTP/ADP ratio and drives basal insulin secretion, at least in part (2, 5). Insulin-secretory profiles of MIN6-GDH266C cells and Islets-GDH266C are in agreement with this hypothesis. Constitutively activated GDH rendered the cells responsive to glutamine in insulin secretion in the absence of luecine and enhanced insulin secretion at low glucose concentrations. Furthermore, they would be reflected in the fasting and protein meal-induced hyperinsulinemic hypoglycemia in patients with HI/HA syndrome, although in patients' β-cells elevation of GDH activity at low glucose concentrations would be modest compared with that in MIN6-GDH266C cells and in Islets-GDH266C. On the other hand, in our previous and present studies, glucose-stimulated insulin secretion was not enhanced in either MIN6-GDH266C cells (22) or Islets-GDH266C (Fig. 3*B*). On the basis of the insulin secretion profiles and glutamate metabolism, our data do not support the hypothesis that glutamate, derived from the reverse GDH reaction (flux from α-ketoglutarate to glutamate), is a second messenger of glucose-stimulated insulin secretion (1, 2, 5, 8, 9), although we neither measured the flux directly nor tested

the messenger action of glutamate in glucose-stimulated insulin secretion, and therefore the messenger role of glutamate is not completely excluded.

This is the first study, to our knowledge, in which insulin secretion and glutamate metabolism were analyzed simultaneously under conditions of direct and constitutive cellular GDH activity elevation. Our results illustrate the importance of GDH in amino acid-stimulated insulin secretion and possible contribution to the regulation of basal insulin secretion. Furthermore, we have provided additional evidence that, at least under our experimental conditions, the metabolic flux through GDH is in the direction of α-ketoglutarate production in pancreatic β-cells. No evidence was obtained to suggest that glutamate produced by the reverse GDH reaction enhanced insulin secretion.

ACKNOWLEDGMENTS

We thank Prof. Jun-ichi Miyazaki, Osaka University, Japan, for providing us with MIN6 cells. We are grateful to Atsuko Tanimura, Yukari Kora-Miura, and Mayumi Kaneko for expert technical assistance.

GRANTS

This study was supported in part by Grants-in-Aid for Creative Scientific Research (10NP0201 to Y. Oka) and for Scientific Research (14370338 to Y. Tanizawa) from the Ministry of Education, Culture, Sports, Science and Technology of Japan.

REFERENCES

1. **Bertrand G, Ishiyama N, Nenquin M, Ravier MA, and Henquin JC.** The elevation of glutamate content and the amplification of insulin secretion in glucose-stimulated pancreatic islets are not causally related. *J Biol Chem* 277: 32883–32891, 2002.
2. **Gao ZY, Li G, Najafi H, Wolf BA, and Matschinsky FM.** Glucose regulation of glutaminolysis and its role in insulin secretion. *Diabetes* 48: 1535–1542, 1999.
3. **Godel H, Graser T, Foldi P, Pfaender P, and Furst P.** Measurement of free amino acids in human biological fluids by high-performance liquid chromatography. *J Chromatogr* 297: 49–61, 1984.
4. **Hoy M, Maechler P, Efanov AM, Wollheim CB, Berggren PO, and Gromada J.** Increase in cellular glutamate levels stimulates exocytosis in pancreatic beta-cells. *FEBS Lett* 531: 199–203, 2002.
5. **Kelly A, Li C, Gao Z, Stanley CA, and Matschinsky FM.** Glutaminolysis and insulin secretion: from bedside to bench and back. *Diabetes* 51, *Suppl* 3: S421–S426, 2002.
6. **Lacy PE and Kostianovsky M.** Method for the isolation of intact islets of Langerhans from the rat pancreas. *Diabetes* 16: 35–39, 1967.
7. **Liu YJ, Cheng H, Drought H, MacDonald MJ, Sharp GW, and Straub SG.** Activation of the K_{ATP} channel-independent signaling pathway by the nonhydrolyzable analog of leucine, BCH. *Am J Physiol Endocrinol Metab* 285: E380–E389, 2003.
8. **MacDonald MJ and Fahien LA.** Glutamate is not a messenger in insulin secretion. *J Biol Chem* 275: 34025–34027, 2000.
9. **MacMullen C, Fang J, Hsu BY, Kelly A, de Lonlay-Debeney P, Saudubray JM, Ganguly A, Smith TJ, and Stanley CA.** Hyperinsulinism/hyperammonemia syndrome in children with regulatory mutations in the inhibitory guanosine triphosphate-binding domain of glutamate dehydrogenase. *J Clin Endocrinol Metab* 86: 1782–1787, 2001.
10. **Maechler P, Gjinovci A, and Wollheim CB.** Implication of glutamate in the kinetics of insulin secretion in rat and mouse perfused pancreas. *Diabetes* 51, *Suppl* 1: S99–S102, 2002.
11. **Maechler P and Wollheim CB.** Mitochondrial glutamate acts as a messenger in glucose-induced insulin exocytosis. *Nature* 402: 685–689, 1999.
12. **Minami K, Yano H, Miki T, Nagashima K, Wang CZ, Tanaka H, Miyazaki JI, and Seino S.** Insulin secretion and differential gene expression in glucose-responsive and -unresponsive MIN6 sublines. *Am J Physiol Endocrinol Metab* 279: E773–E781, 2000.
13. **Miyazaki J, Araki K, Yamato E, Ikegami H, Asano T, Shibasaki Y, Oka Y, and Yamamura K.** Establishment of a pancreatic beta cell line that retains glucose-inducible insulin secretion: special reference to expression of glucose transporter isoforms. *Endocrinology* 127: 126–132, 1990.
14. **Mizuguchi H and Kay MA.** Efficient construction of a recombinant adenovirus vector by an improved in vitro ligation method. *Hum Gene Ther* 9: 2577–2583, 1998.
15. **Mizuguchi H and Kay MA.** A simple method for constructing E1- and E1/E4-deleted recombinant adenoviral vectors. *Hum Gene Ther* 10: 2013–2017, 1999.
16. **Peterson PE and Smith TJ.** The structure of bovine glutamate dehydrogenase provides insights into the mechanism of allostery. *Structure Fold Des* 7: 769–782, 1999.
17. **Rubi B, Ishihara H, Hegardt FG, Wollheim CB, and Maechler P.** GAD65-mediated glutamate decarboxylation reduces glucose-stimulated insulin secretion in pancreatic beta cells. *J Biol Chem* 276: 36391–36396, 2001.
18. **Sener A and Malaisse WJ.** L-Leucine and a nonmetabolized analogue activate pancreatic islet glutamate dehydrogenase. *Nature* 288: 187–189, 1980.
19. **Sener A, Malaisse-Lagae F, and Malaisse WJ.** Stimulation of pancreatic islet metabolism and insulin release by a nonmetabolizable amino acid. *Proc Natl Acad Sci USA* 78: 5460–5464, 1981.
20. **Stanley CA, Fang J, Kutyna K, Hsu BY, Ming JE, Glaser B, and Poncz M.** Molecular basis and characterization of the hyperinsulinism/hyperammonemia syndrome: predominance of mutations in exons 11 and 12 of the glutamate dehydrogenase gene. HI/HA Contributing Investigators. *Diabetes* 49: 667–673, 2000.
21. **Stanley CA, Lieu YK, Hsu BY, Burlina AB, Greenberg CR, Hopwood NJ, Perlman K, Rich BH, Zammarchi E, and Poncz M.** Hyperinsulinism and hyperammonemia in infants with regulatory mutations of the glutamate dehydrogenase gene. *N Engl J Med* 338: 1352–1357, 1998.
22. **Tanizawa Y, Nakai K, Sasaki T, Anno T, Ohta Y, Inoue H, Matsuo K, Koga M, Furukawa S, and Oka Y.** Unregulated elevation of glutamate dehydrogenase activity induces glutamine-stimulated insulin secretion: identification and characterization of a GLUD1 gene mutation and insulin secretion studies with MIN6 cells overexpressing the mutant glutamate dehydrogenase. *Diabetes* 51: 712–717, 2002.
23. **Tanizawa Y, Ohta Y, Nomiyama J, Matsuda K, Tanabe K, Inoue H, Matsutani A, Okuya S, and Oka Y.** Overexpression of dominant negative mutant hepatocyte nuclear factor (HNF)-1alpha inhibits arginine-induced insulin secretion in MIN6 cells. *Diabetologia* 42: 887–891, 1999.
24. **Ueda K, Tanizawa Y, Ishihara H, Kizuki N, Ohta Y, Matsutani A, and Oka Y.** Overexpression of mitochondrial FAD-linked glycerol-3-phosphate dehydrogenase does not correct glucose-stimulated insulin secretion from diabetic GK rat pancreatic islets. *Diabetologia* 41: 649–653, 1998.
25. **Weinzimer SA, Stanley CA, Berry GT, Yudkoff M, Tuchman M, and Thornton PS.** A syndrome of congenital hyperinsulinism and hyperammonemia. *J Pediatr* 130: 661–664, 1997.
26. **Wrzeszczynski KO and Colman RF.** Activation of bovine liver glutamate dehydrogenase by covalent reaction of adenosine 5′-O-[S-(4-bromo-2,3-dioxobutyl)thiophosphate] with arginine-459 at an ADP regulatory site. *Biochemistry* 33: 11544–11553, 1994.
27. **Yamada H, Yamamoto A, Yodozawa S, Kozaki S, Takahashi M, Morita M, Michibata H, Furuichi T, Mikoshiba K, and Moriyama Y.** Microvesicle-mediated exocytosis of glutamate is a novel paracrine-like chemical transduction mechanism and inhibits melatonin secretion in rat pinealocytes. *J Pineal Res* 21: 175–191, 1996.
28. **Yamada S, Komatsu M, Sato Y, Yamauchi K, Aizawa T, and Hashizume K.** Glutamate is not a major conveyer of ATP-sensitive K+ channel-independent glucose action in pancreatic islet beta cell. *Endocr J* 48: 391–395, 2001.
29. **Zammarchi E, Filippi L, Novembre E, and Donati MA.** Biochemical evaluation of a patient with a familial form of leucine-sensitive hypoglycemia and concomitant hyperammonemia. *Metabolism* 45: 957–960, 1996.

K. Takahashi
J. Satoh
Y. Kojima
K. Negoro
M. Hirai
Y. Hinokio
Y. Kinouchi
S. Suzuki
N. Matsuura
T. Shimosegawa
Y. Oka

Promoter polymorphism of *SLC11A1* (formerly *NRAMP1*) confers susceptibility to autoimmune type 1 diabetes mellitus in Japanese

Key words:
antigen-presenting cells; insulin-dependent diabetes mellitus; macrophage activation; macrophages; natural resistance; NRAMP; polymorphism; SLC11A1

Acknowledgments:
We thank Ms C. Suzuki for technical assistance. This study was supported by a grant-in-aid for Scientific Research on Priority Areas (C) 'Medical Genome Science' from the Ministry of Education, Culture, Sports, Science and Technology of Japan (to YO) and grants from the Japan Society for the Promotion of Science (14570401), the Takeda Medical Research Foundation, and the Japan Insulin Study Group Foundation (to KT).

Abstract: Defective function of antigen-presenting cells has been postulated to be one of the non-HLA-linked susceptibility factors for type 1 diabetes mellitus, though the underlying genetic factors remain unclear. SLC11A1 (formerly NRAMP1), a divalent cation transporter, plays a crucial role in macrophage activation. We performed a case-control study in 224 healthy and 95 type 1 diabetic Japanese subjects, examining the length polymorphisms in the promoter region (−377 to −222) of *SLC11A1*, which may influence transcriptional activity. Alleles designated 2, 3, and 7 have been identified in Japanese subjects. The frequency of allele 7 was significantly higher in subjects with type 1 diabetes (9.47%) than in the healthy controls (4.46%). The difference is more marked in the subpopulation of Japanese subjects with type 1 diabetes; diabetic subjects with at least one protective HLA class II allele and those without any susceptibility HLA class II haplotypes, DR4-DQ4 or DR9-DQ9, had a much higher allele 7 frequency than controls. These findings suggest that the novel promoter polymorphism of *SLC11A1* influences the susceptibility to type 1 diabetes in Japanese subjects.

Authors' affiliation:

K. Takahashi[1]
J. Satoh[1]
Y. Kojima[2]
K. Negoro[2]
M. Hirai[1]
Y. Hinokio[1]
Y. Kinouchi[2]
S. Suzuki[1]
N. Matsuura[3]
T. Shimosegawa[2]
Y. Oka[1]

[1]Division of Molecular Metabolism and Diabetes, Department of Internal Medicine, Tohoku University Graduate School of Medicine, Sendai, Japan

[2]Division of Gastroenterology, Department of Internal Medicine, Tohoku University Graduate School of Medicine, Sendai, Japan

[3]Department of Pediatrics, Kitasato University School of Medicine, Sagamihara, Japan

Correspondence to:
Dr Kazuma Takahashi, MD, PhD
Division of Molecular Metabolism and Diabetes
Tohoku University Graduate School of Medicine
1-1 Seiryo-machi, Aoba-ku
Sendai 980-8574, Japan
Tel.: +81-22-717-7171
Fax: +81-22-717-7177
e-mail: ktakahashi@int3.med.tohoku.ac.jp

Antigen-presenting cells (APCs) strongly influence several qualitative and quantitative aspects of T-cell activation (1–4). In humans at risk for type 1 diabetes mellitus and in the non-obese diabetic (NOD) mouse, the murine model for this disease, defects in APCs contribute to low levels of T-cell activation, poor interleukin-2 (IL-2) production, and deficient activation of regulatory T cells (5–8). Defective APC function may predispose to autoimmunity through reduction in signals required for activation-induced T-cell death or regulatory T-cell responses, both of which are important mechanisms for peripheral tolerance (3, 9, 10). Factors contributing to APC dysfunction in type 1 diabetes in humans and in NOD mouse include those encoded by the major histocompatibility complex (MHC) class II region and non-MHC alleles. The unique H-2^{g7} molecule of the NOD mouse plays a central role, as the inability of NOD APCs to activate immunoregulatory T cells in a syngeneic mixed lymphocyte reaction was associated with the homozygous expression of H-2^{g7} (11), and

Received 21 May 2003, revised 11 September 2003, accepted 30 September 2003

Tissue Antigens 2004: **63:** 231–236
Printed in Denmark.

marrow-derived APCs from NOD congenic mice expressing the diabetes-resistant H-2^{nb1} haplotype of NOD mice inhibited the development of diabetogenic T cells from NON marrow (12). In addition to the MHC, multiple non-MHC-susceptibility genes contribute to the pathogenesis of insulin-dependent diabetes mellitus (IDDM) in the NOD mouse and in humans (13). The identities of these genes and their contributions to APC dysfunction however have not been defined.

SLC11A1 (formerly NRAMP1), a divalent cation transporter (14), plays important roles early in the macrophage activation and displays multiple pleiotropic effects on macrophage function, including the expression of chemokines, IL-1β, tumor necrosis factor α-inducible nitric oxide synthase, and MHC class II molecules (14). *SLC11A1* is located on human chromosome 2 (2q35), which includes at least three human type 1 diabetes-susceptible loci [*IDDM7* (15), *IDDM12* (16), and *IDDM13* (17)]. Several candidate genes in this region have already been focused on in several association studies carried out on various genetic backgrounds, and association of *CTLA-4* (18) in *IDDM12* and of *NeuroD/BETA2* (19) in *IDDM13* with type 1 diabetes has been suggested in Japanese. However, the multiple pleiotropic effect of SLC11A1 on macrophage function, as well as the report by Hill et al. (20) that proposed SLC11A1 as a prime candidate for a mouse type 1 diabetes locus, *Idd5.2*, the homolog of human *IDDM13*, prompted us to look for association of *SLC11A1* with human type 1 diabetes mellitus.

In the promoter region of *SLC11A1*, six different alleles of the polymorphism have been reported at functional Z-DNA forming repeats in Caucasian. Several studies support the hypothesis that this functional repeat polymorphism contributes to the susceptibility to autoimmune and infectious diseases. In rheumatoid arthritis and juvenile rheumatoid arthritis, family-based transmission disequilibrium testing or case-control analyses have all shown an allelic association with allele 3, possessing the strongest activity driving the SLC11A1 expression, while allele 2 with weaker promoter activity is significantly protective. Conversely, allele 2 displays positive association with infectious diseases including tuberculosis and leprosy and is protective in autoimmune diseases (14). So far, the association of allele 2 and allele 3 in *SLC11A1* polymorphism with type 1 diabetes mellitus is limited; allele 2 is negatively associated with a subpopulation of early-onset type 1 diabetes in Japanese, but not with whole population (21), and allele 3 was significantly transmitted to type 1 diabetic siblings in UK families that have a first- or second-degree relative with rheumatoid arthritis (22).

Recently, Kojima et al. identified the allele with 15 GT repeats in Japanese (23). This novel allele, named allele 7, is the same in length as, but different in sequences from, allele 1 reported in Caucasians. Contrary to the previous observations on autoimmune diseases, they could confirm neither positive association of allele 3 nor negative association of allele 2 with inflammatory bowel diseases, but found allele 7 susceptible. In the present study, we have extended their observation on Inflammatory Bowel Disease (IBD) to type 1 diabetes mellitus and performed a case-control study to explore the pathogenic role of the *SLC11A1*-promoter polymorphism in type 1 diabetes mellitus in Japanese.

Materials and methods

Subjects

After obtaining approval from the ethics committee of the Tohoku University Graduate School of Medicine and informed consent from all subjects, blood samples were collected from 224 healthy subjects (115 males and 109 females), and 95 type 1 diabetic subjects (43 males and 52 females). Mean age at onset (±SD) was 15.7 ± 11.1 years (range 1–36 years). All the subjects were Japanese. All type 1 diabetic subjects were ketosis prone, insulin dependent since diagnosis, and positive for either autoantibody to glutamic acid decarboxylase (GAD) or insulinoma-associated protein-2 (IA-2). The mean ages (±SD) of control and diabetic subjects were 29.5 ± 12.1 and 27.6 ± 11.8 years, respectively.

Autoantibodies

Anti-GAD autoantibody was assayed using an immunoassay kit, GAD Ab Cosmic (Cosmic, Tokyo, Japan) (24). Anti-tyrosine phosphatase IA-2 autoantibody was measured by precipitation of [^{35}S] methionine-labeled recombinant proteins synthesized after transcription translation in a TNT^{TM}-coupled reticulocyte lysate system (Promega, Madison, WI) (5).

Determination of length polymorphisms and identification of their corresponding sequences

Genomic DNAs were obtained from peripheral blood leucocytes by standard phenol–chloroform extraction and ethanol precipitation or by utilizing an NA-1000 Automated Nucleic Acid Extraction Machine (Kurabo, Osaka, Japan). To identify the polymorphism, the promoter region spanning −377 to −222 relative to the transcription start site was amplified by polymerase chain reaction (PCR) using a thermal cycler (Perkin-Elmer, Foster City, CA). The PCR primers were as follows: 5′hexachlorofluorescein (HEX)-labeled sense (HEX-NRAMP-S1), 5′-CATTAGGCCAACGAGGGGTCTT-3′; and non-labeled antisense (NRAMP-as1), 5′-TCCTGCCCCTTGCGTATTCATG-3′. PCR conditions were as follows: 45 cycles of denaturing at

94°C for 30 s, annealing at 65°C for 2 min, extension at 72°C for 3 min with a final incubation at 72°C for 10 min. The lengths of the PCR products were determined with an ABI 310 Genetic Analyser and computer software, Genescan and Sequencing Analysis (Perkin-Elmer Biosystems). Sequences of seven alleles of this polymorphism were as follows: allele 1 (160 bp), t(gt)5ac(gt)5ac(gt)11ggcaga(g)6; allele 2 (158 bp), t(gt)5ac (gt)5ac(gt)10ggcaga(g)6; allele 3 (156 bp), t(gt)5ac(gt)5ac(gt)9ggcaga(g)6; allele 4 (144 bp), t(gt)5ac(gt)9ggcaga(g)6; allele 5 (156 bp), t(gt)4ac(gt) 5ac(gt)10ggcaga(g)6; allele 6 (157 bp), t(gt)5ac(gt)5ac(gt)4at(gt)4ggcaga(g)7; allele 7 (160 bp), t(gt)5ac(gt)5at(gt)11ggcaga(g)6. Only alleles 2, 3, and 7 are observed in Japanese (23). The correspondence between the length and the sequence of each PCR product has been confirmed using PCR cycle sequencing by Kojima et al. (23).

HLA typing

A subset of patients ($n = 54$) were genotyped for HLA-DQA1, HLA-DQB1, and HLA-DRB1. Alleles were determined by the PCR-restriction fragment length polymorphism method (25). The most probable HLA-DR and HLA-DQ haplotypes were deduced from known linkage disequilibria (26).

Statistical analysis

Genotype and allele frequencies were calculated by direct counting. Allele frequencies were initially compared between the disease group and the healthy controls with a χ^2 test, if applicable, using a 3×2 contingency table. Each allele was then analyzed using a 2×2 contingency table with a χ^2 test or a Fisher's exact probability test. P was corrected by the number of alleles ($n = 3$) observed in the Japanese population (Table 1). In analyzing *SLC11A1* polymorphism in terms of *HLA* genotype, P was corrected 3 times 30, the number of HLA DR-DQ haplotypes observed. P- or Pc (corrected P)-values <0.05 were considered to be statistically significant. The strength of association was estimated by the odds ratio.

Results

In all Japanese subjects examined, three alleles, alleles 2, 3, and 7, were identified in the *SLC11A1*-promoter region, while alleles 1, 4, 5, and 6 were not. These results were consistent with those of the previous studies on Japanese subjects (23). Gender and age did not affect allele frequencies of this polymorphism (data not shown). Allele 7 was noted to be positively associated with type 1 diabetes ($P = 0.03$ and $Pc = 0.042$, with a χ^2 test using 2×2 and 3×2 contingency tables, respectively) (Table 1). The frequency of alleles 2 and 3 did not differ between the type 1 diabetic subjects and controls with a Bonferroni multiple adjustment using a 2×2 contingency table (Table 1).

Because the HLA gene (*IDDM1*) exerts the greatest influence on the susceptibility to type 1 diabetes, association of the *SLC11A1* polymorphism with diabetes was analyzed in terms of the *IDDM1* genotype. A subset of the subjects with diabetes ($n = 54$) were analyzed for HLA class II genotype, and this subpopulation was employed for further analysis. The *HLA* allele frequencies in this subpopulation were similar to those of a recent Japanese report (27) (data not shown). In addition, the *SLC11A1* allele frequencies of this subpopulation (allele 2, 9.4%; allele 3, 80.2%; allele 7, 10.4%) were very similar to those of whole type 1 diabetic population (allele 2, 11.6%; allele 3, 78.9%; allele 7, 9.5%). This subpopulation was stratified according to the presence of susceptibility, neutral, and protective alleles for *IDDM1*. The diabetic subjects with high-risk HLA haplotypes, DR4-DQ4/X ($n = 16$, X does not contain DR9-DQ9 or protective alleles), DR9-DQ9/Y ($n = 16$, Y does not contain DR4-DQ4 or protective alleles), or DR4-DQ4/DR9-DQ9 ($n = 5$), did not show a significant difference in the allele distribution of *SLC11A1*, as compared with the controls. On the contrary, the rest ($n = 17$) of the diabetic subjects with at least one protective allele, DRB1*0601, in combination with any haplotype, and those without any susceptibility haplotypes had a much higher allele 7 frequency (23.5%) than the controls (4.5%) ($Pc = 0.0042$, Fisher's exact probability test) (Table 2).

Allele frequencies of polymorphisms in the promoter region of SLC11A1

Allele	Subject	Allele frequency (%)	Odds ratio	95% CI	*Pc* by 2×2 χ^2 test	*P* by 2×3 χ^2 test
2	Type 1 diabetes ($n = 95$)	11.6	0.72	0.43–1.2	0.62	
	Control ($n = 224$)	15.4				
3	Type 1 diabetes ($n = 95$)	78.9	0.93	0.61–1.4	2.2	
	Control ($n = 224$)	80.1				
7	Type 1 diabetes ($n = 95$)	9.47	2.2	1.2–4.3	0.042	0.030
	Control ($n = 224$)	4.46				

Table 1

Allele frequencies of the SLC11A1-promoter polymorphisms in the HLA-genotyped subjects with type 1 diabetes mellitus

Allele	Subject	Allele frequency (%)	Odds ratio	95% CI	*Pc*[a]
2	HLA-genotyped patients ($n=54$)	9.43	0.57	0.29–1.1	0.33
	DR4-DQ4/X ($n=16$)	10.7	0.57	0.17–1.9	24[b]
	DR9-DQ9/Y ($n=16$)	10.7	0.57	0.17–1.9	24[b]
	DR4-DQ4/DR9-DQ9 ($n=5$)	20.0	1.37	0.29–6.6	42[b]
	Any/P or N/N ($n=17$)	5.88	0.34	0.090–1.4	8.7[b]
	Control ($n=224$)	15.4			
3	HLA-genotyped patients ($n=54$)	80.2	1.0	0.59–1.7	3.0
	DR4-DQ4/X ($n=16$)	87.5	1.7	0.65–3.1	33[b]
	DR9-DQ9/Y ($n=16$)	81.3	1.1	0.43–2.7	78[b]
	DR4-DQ4/DR9-DQ9 ($n=5$)	80.0	1.0	0.21–4.8	63[b]
	Any/P or N/N ($n=17$)	70.6	0.6	0.28–1.3	78[b]
	Control ($n=224$)	80.1			
7	HLA-genotyped patients ($n=54$)	10.4	2.5	1.2–23	0.017
	DR4-DQ4/X ($n=16$)	3.13	0.69	0.090–5.3	54[b]
	DR9-DQ9/Y ($n=16$)	10.7	2.2	0.64–7.7	17[b]
	DR4-DQ4/DR9-DQ9 ($n=5$)	0.00	0.0		57[b]
	Any/P or N/N ($n=17$)	23.5	6.6	2.9–15	0.0042[b]
	Control ($n=224$)	4.46			

[a]Fischer's exact test was used, when χ^2 test was not applicable.
[b]*P* was corrected 3 times 30, the number of SLC11A1 alleles and *HLA* DR-DQ haplotypes observed, respectively.
N, neutral alleles; P, protective alleles; X, not containing DR9-DQ9 or protective alleles; Y, not containing DR4-DQ4 or protective alleles.

Table 2

Discussion

To our knowledge, this is the first report to show an association of type 1 diabetes with allele 7 of the *SLC11A1*-promoter polymorphism. Kojima et al. (23) recently identified allele 7 in Japanese, which has the same length with, but different sequence from, allele 1 and also showed the absence of allele 1 in Japanese. The *SLC11A1*-promoter polymorphism in a Japanese population was previously determined only by length, but not by sequences (21, 28, 29). Because alleles 1 and 7 are the same in length but different in sequence, the allele 1 in these reports must be allele 7.

In Caucasians, stronger promoter activity of allele 3 to drive higher SLC11A1 expression than other alleles leads to the hypothesis that the high expression of SLC11A1 promoted by allele 3 may produce chronic macrophage hyperactivation, causing autoimmune diseases (14). The activity of allele 7 has not been determined so far, and hence we cannot interpret our present data in functional regards. Similar to allele 1, which reportedly has low promoter activity in Caucasian, allele 7 also has 11 GT repeats. The length is the same and the sequences are basically similar between allele 1 and allele 7. These two alleles, however, possibly are different in their ability to drive gene expression, because a single-nucleotide substitution in the promoter region of a gene can alter transcriptional efficiency (30–32). Positive association of allele 7 with Crohn's disease, ulcerative colitis (23), and Kawasaki disease (28), in which chronic activation of monocytes/macrophages and consequent high production of monokines play key roles, lead us to surmise that this allele possesses strong activity to drive SLC11A1 expression. A functional study of this allele is necessary to shed light on the association of allele 7 with type 1 diabetes.

Our present results are not completely in line with a recent report by Bassuny et al. (21) that showed negative association of allele 2 with early-onset type 1 diabetic subjects in Japanese, although the difference did not reach statistical significance. In our study, the frequencies of allele 2, 3, and 7 were 15, 74, and 11%, respectively in early-onset subpopulation (age of onset, <10, $n=120$, $P=0.11$ by χ^2 test) and 5.7, 87, and 7.1% respectively in late-onset subpopulation (age of onset, >10, $n=70$). In whole type 1 diabetic subjects, allele 2 frequency was significantly lower with a χ^2 test using a 3×2 contingency table, but not with a Bonferroni multiple adjustment using a 2×2 contingency table (Table 1). The negative association of allele 2 with type 1 diabetes needs to be validated in Japanese population,

because this would uphold the hypothesis in Caucasians; the lower SLC11A1 expression level promoted by allele 2 leads to insufficient activation of macrophages, thereby enhancing resistance to autoimmune diseases.

We found allele 7 as a culprit, but Bassuny et al. (21) did not. Control subjects in their report displayed higher allele 7 frequency (8.2%) than ours and other previous reports conducted in an East Asian population. Allele 7 frequency of our control subjects, 4.5% in Sendai, seems more likely as one of those observed in East Asia; 2.2, 3.2, and 4.0 in Tokyo and Osaka (29), Kawasaki (28), and Korea (33), respectively.

It is noteworthy that this polymorphism showed much stronger association with type 1 diabetes in the subpopulation of those lacking one of two diabetes-susceptibility HLA haplotypes and those possessing at least one protective allele. This observation is similar to previous findings on *IDDM13* in Caucasian (17) and Japanese (34) subjects; a stronger association of type 1 diabetes with the *IDDM13* gene was observed in subjects without the major susceptibility HLA alleles. This may explain why we detected a significant contribution of *SLC11A1* in a case-control study in Japanese. Because Japanese have a lower frequency of strong susceptibility *HLA* haplotypes than Caucasians, the contribution of *SLC11A1* to type 1 diabetes susceptibility may be easier to detect.

Although it is possible that the *SLC11A1* polymorphism is directly involved in the predisposition to type 1 diabetes, other possibilities including linkage disequilibrium of this polymorphism with a susceptibility gene remain to be elucidated. In proximity to the *SLC11A1* are several genes which has been suggested to be involved in the pathogenesis of this disease, including IL-8 receptor α and β and caspase 8 genes.

In summary, allele 7 of the *SLC11A1* is an important predisposing factor for type 1 diabetes development especially in the Japanese population. These observations should be examined in other especially Asians ethnic populations.

References

1. Ashton-Rickardt PG, Bandeira A, Delaney JR et al. Evidence for a differential avidity model of T cell selection in the thymus. *Cell* 1994: **76**: 651–63.
2. Rocha B, von Boehemer H. Peripheral selection of the T cell repertoire. *Science* 1991: **251**: 1225–31.
3. Ucker DS, Meyers J, Obermiller PS. Activation-driven T cell death. II. Quantitative differences alone distinguish stimuli triggering nontransformed T cell proliferation or death. *J Immunol* 1993: **149**: 1583–92.
4. Critchfield JM, Racke MK, Zuniga-Pflucker JC et al. T cell deletion in high antigen dose therapy of autoimmune encephalomyelitis. *Science* 1994: **263**: 1139–43.
5. Takahashi K, Honeyman MC, Harrison LC. Impaired yield, phenotype, and function of monocyte-derived dendritic cells in humans at risk for insulin-dependent diabetes. *J Immunol* 1998: **161**: 2629–35.
6. Yokono K, Kasase Y, Nagata M, Hatamori N, Baba S. Suppression of concanavalin A-induced responses in splenic lymphocytes by activated macrophages in the non-obese diabetic mouse. *Diabetologia* 1989: **32**: 67–73.
7. Smerdon RA, Peakman M, Hussain MJ et al. Increase in simultaneous coexpression of naive and memory lymphocyte markers at diagnosis of IDDM. *Diabetes* 1993: **42**: 127–33.
8. Serreze DV, Gaskins HR, Leiter EH. Defective activation of T suppressor cell function in nonobese diabetic mice: potential relationship to cytokine deficiencies. *J Immunol* 1993: **150**: 2534–43.
9. Milich DR, Jones JE, McLachlan A, Houghten R, Thornton GB, Hughes JL. Distinction between immunogenicity and tolerogenicity among HBcAg T cell determinants. Influence Peptide–MHC Interaction. *J Immunol* 1989: **143**: 3148–56.
10. Mamula MJ. The inability to process a self-peptide allows autoreactive T cells to escape tolerance. *J Exp Med* 1993: **17**: 567–71.
11. Serreze DV, Leiter EH. Defective activation of T suppressor cell function in nonobese diabetic mice: potential relation to cytokine deficiencies. *J Immunol* 1988: **140**: 3801–7.
12. Serreze DV, Leiter EH. Development of diabetogenic T cells from NOD/Lt marrow is blocked when an allo-H-2 haplotype is expressed on cells of hemopoietic origin, but not on thymic epithelium. *J Immunol* 1991: **147**: 1222–9.
13. Merriman TR, Todd JA. Genetics of insulin-dependent diabetes: non-major histocompatibility genes. *Horm Metab Res* 1996: **28**: 289–93.
14. Searle S, Blackwell JM. Evidence for a functional repeat polymorphism in the promoter of the human SLC11A1 gene that correlates with autoimmune versus infectious disease susceptibility. *J Med Genet* 1999: **36**: 295–9.
15. Copeman JB, Cucca F, Hearne CM et al. Linkage disequilibrium mapping of a type 1 diabetes susceptibility gene (IDDM7) to chromosome 2q31-q33 Nat Genet. 1995: 9: 80–5.
16. Nistico L, Buzzetti R, Pritchard LE et al. The CTLA-4 gene region of chromosome 2q33 is linked to, and associated with, type 1 diabetes. *Hum Mol Genet* 1996: **5**: 1075–80.
17. Morahan G, Huang D, Tait BD, Colman PG, Harrison LC. Markers on distal chromosome 2q linked to insulin-dependent diabetes mellitus. *Science* 1996: **272**: 1811–3.
18. Awata T, Kurihara S, Iitaka M et al. Association of CTLA-4 gene A-G polymorphism (IDDM12 locus) with acute-onset and insulin-depleted IDDM as well as autoimmune thyroid disease (Graves' disease and Hashimoto's thyroiditis) in the Japanese population. *Diabetes* 1998: **47**: 128–9.
19. Iwata I, Nagafuchi S, Nakashima H et al. Association of polymorphism in the NeuroD/BETA2 gene with type 1 diabetes in the Japanese. *Diabetes* 1999: **48**: 416–9.

20. Hill NJ, Lyons PA, Armitage N, Todd JA, Wicker LS, Peterson LB. NOD Idd5 locus controls insulitis and diabetes and overlaps the orthologous CTLA4/IDDM12 and SLC11A1 loci in humans. *Diabetes* 2000: **49**: 1744–7.
21. Bassuny WM, Ihara K, Matsuura N et al. Association study of the NRAMP1 gene promoter polymorphism and early-onset type 1 diabetes. *Immunogenetics* 2002: **54**: 282–5.
22. Esposito L, Hill NJ, Pritchard LE et al. Genetic analysis of chromosome 2 in type 1 diabetes: analysis of putative loci IDDM7, IDDM12, and IDDM13 and candidate genes NRAMP1 and IA-2 and the interleukin-1 gene cluster. IMDIAB Group. *Diabetes* 1998: **47**: 1797–9.
23. Kojima Y, Kinouchi K, Takahashi S et al. Inflammatory bowel disease is associated with a novel promoter polymorphism of SLC11A1 gene. *Tissue Antigens* 2001: **58**: 379–84.
24. Bando Y, Ushiogi Y, Toya D, Tanaka N, Fujisawa M. Antibodies to glutamic acid decarboxylase (GAD) in non-obese Japanese diabetics without insulin therapy: a comparison of two commercial RIA kits based on recombinant and pig brain GAD. *Diabetes Res Clin Pract* 1998: **41**: 25–33.
25. Bidwell J. DNA-RFLP analysis and genotyping of HLA-DR and DQ antigens. *Immunol Today* 1988: **9**: 18–23.
26. Imahashi T, Akaza T, Kimura A, Tokunaga K, Gojobori T. Allele and haplotype frequencies for HLA and complement loci in various ethnic groups. In: Tsuji K, Aizawa M, Sasazuki T, eds. *HLA 1991: Proceedings of the Eleventh International Histocompatibility Workshop and Conference*. Oxford: Oxford University Press, 1992: 1065–220.
27. Kawabata Y, Ikegami H, Kawaguchi Y et al. Asian-specific HLA haplotypes reveal heterogeneity of the contribution of HLA-DR and -DQ haplotypes to susceptibility to type 1 diabetes. *Diabetes* 2002: **51**: 545–51.
28. Ouchi K, Suzuki Y, Shirakawa T, Kishi F. Polymorphism of SLC11A1 (formerly NRAMP1) gene confers susceptibility to Kawasaki disease. *J Infect Dis* 2003: **187**: 326–9.
29. Gao PS, Fujishima S, Mao XQ et al. Genetic variants of NRAMP1 and active tuberculosis in Japanese populations. International Tuberculosis Genetics Team. *Clin Genet* 2000: **58**: 74–6.
30. Fishman D, Faulds G, Jeffery R et al. The effect of novel polymorphisms in the interleukin-6 (IL-6) gene on IL-6 transcription and plasma IL-6 levels, and an association with systemic-onset juvenile chronic arthritis. *J Clin Invest* 1998: **102**: 1369–76.
31. Li LC, Chui RM, Sasaki M et al. A single nucleotide polymorphism in the E-cadherin gene promoter alters transcriptional activities. *Cancer Res* 2000: **60**: 873–6.
32. Crawley E, Kay R, Sillibourne J, Patel P, Hutchinson I, Woo P. Polymorphic haplotypes of the interleukin-10 5′ flanking region determine variable interleukin-10 transcription and are associated with particular phenotypes of juvenile rheumatoid arthritis. *Arthritis Rheum* 1999: **42**: 1101–8.
33. Yang YS, Kim SJ, Kim JW, Koh EM. NRAMP1 gene polymorphisms in patients with rheumatoid arthritis in Koreans *J Korean Med Sci* 2000: **15**: 83–7.
34. Fu J, Ikegami H, Kawaguchi Y et al. Association of distal chromosome 2q with IDDM in Japanese subjects. *Diabetologia* 1998: **41**: 228–32.

Human Molecular Genetics, 2004, Vol. 13, No. 11 **1159–1170**
DOI: 10.1093/hmg/ddh125
Advance Access published on March 31, 2004

Disruption of the *WFS1* gene in mice causes progressive β-cell loss and impaired stimulus–secretion coupling in insulin secretion

Hisamitsu Ishihara[1], Satoshi Takeda[4], Akira Tamura[1], Rui Takahashi[1], Suguru Yamaguchi[1], Daisuke Takei[1], Takahiro Yamada[1], Hiroshi Inoue[5], Hiroyuki Soga[2], Hideki Katagiri[3], Yukio Tanizawa[6] and Yoshitomo Oka[1,*]

[1]Division of Molecular Metabolism and Diabetes, [2]Division of Immunology and Embryology, and [3]Division of Advanced Therapeutics for Metabolic Diseases, Tohoku University Graduate School of Medicine, Sendai, Japan, [4]Otsuka GEN Research Institute, Otsuka Pharmaceutical Co., Tokushima, Japan, [5]Division of Diabetes and Endocrinology, Department of Medicine, Kawasaki Medical School, Kurashiki, Japan and [6]Division of Molecular Analysis of Human Disorders, Department of Bio-Signal Analysis, Yamaguchi University Graduate School of Medicine, Ube, Japan

Received February 8, 2004; Revised and Accepted March 26, 2004

Wolfram syndrome, an autosomal recessive disorder characterized by juvenile-onset diabetes mellitus and optic atrophy, is caused by mutations in the *WFS1* gene. In order to gain insight into the pathophysiology of this disease, we disrupted the *wfs1* gene in mice. The mutant mice developed glucose intolerance or overt diabetes due to insufficient insulin secretion *in vivo*. Islets isolated from mutant mice exhibited a decrease in insulin secretion in response to glucose. The defective insulin secretion was accompanied by reduced cellular calcium responses to the secretagogue. Immunohistochemical analyses with morphometry and measurement of whole-pancreas insulin content demonstrated progressive β-cell loss in mutant mice, while the α-cell, which barely expresses WFS1 protein, was preserved. Furthermore, isolated islets from mutant mice exhibited increased apoptosis, as assessed by DNA fragment formation, at high concentration of glucose or with exposure to endoplasmic reticulum-stress inducers. These results strongly suggest that WFS1 protein plays an important role in both stimulus–secretion coupling for insulin exocytosis and maintenance of β-cell mass, deterioration of which leads to impaired glucose homeostasis. These WFS1 mutant mice provide a valuable tool for understanding better the pathophysiology of Wolfram syndrome as well as WFS1 function.

INTRODUCTION

Wolfram syndrome (OMIM 222300) is a rare autosomal recessive disorder characterized by juvenile-onset non-autoimmune diabetes mellitus, optic atrophy, sensorineural deafness and diabetes insipidus (1). In addition, psychiatric illnesses such as depression and impulsive behavior are frequently observed in affected individuals (2). The nuclear gene responsible for this syndrome was identified by us (3) and others (4), and designated *WFS1* (3). More than 100 mutations of the *WFS1* gene have been identified to date in Wolfram syndrome patients. Most are inactivating mutations, suggesting loss of function to be responsible for the disease phenotype (5). WFS1 mutations underlie not only autosomal recessive Wolfram syndrome but also autosomal dominant low-frequency sensorineural hearing loss (LFSNHL). Heterozygous, non-inactivating WFS1 mutations were recently found in families with LFSNHL linked to chromosome 4p16 (DFNA6/14/38) (OMIM 600965) (6,7). The observation that the first-degree relatives of Wolfram syndrome patients have increased frequencies of diabetes mellitus and certain psychiatric disorders suggests sequence variants of the *WFS1* gene predispose these individuals to such conditions (2,8). Indeed, several WFS1 sequence variants have been shown to be significantly associated with more common forms of diabetes mellitus (9,10) as well as with suicidal and impulsive behavior (11).

*To whom correspondence should be addressed at: Division of Molecular Metabolism and Diabetes, Tohoku University Graduate School of Medicine, 2-1 Seiryo-machi, Aoba-ku, Sendai 980-8575, Japan. Tel: +81 227177173; Fax: +81 227177179; Email: oka@int3.med.tohoku.ac.jp

The WFS1 protein, also called wolframin (4), consists of 890 amino acids and was predicted to have nine or ten membrane spanning domains (3,4). Proteins with sequence similarity are now found in public databases of other organisms, *Drosophila melanogaster* (CG4917), *Anopheles gambiae* (EBIP3764) and *Fugu rubripes* (SINFRUP82345), but little is known about their functions, suggesting WFS1 protein to belong to a novel family. The WFS1 protein is expressed in various tissues but at higher levels in the brain, heart, lung and pancreas (3,4). We showed the WFS1 protein to be localized predominantly in the endoplasmic reticulum (ER) and suggested a possible role of this protein in membrane trafficking, protein processing and/or regulation of cellular calcium homeostasis (12). A recent study showed this protein to contain nine transmembrane domains and to be embedded in the ER membrane with the amino-terminus in the cytosol and the carboxy-terminus in the ER lumen (13). ER dysfunction is known to cause apoptosis, which underlies a number of genetic disorders (14,15), possibly including a subset of diabetes (15). Since severe atrophic changes have been reported in the brain and in pancreatic islets of subjects with Wolfram syndrome (16,17), it is reasonable to speculate that WFS1 protein plays an essential role in the survival of neuronal cells and islet β-cells.

In this study, to gain insight into the pathophysiology of Wolfram syndrome, we disrupted the *wfs1* gene in mice. The mice developed glucose intolerance or overt diabetes, depending on their genetic background. Our results demonstrate that the impaired glucose homeostasis in these mice results from insufficient insulin secretion due to defects in both stimulus–secretion coupling and maintenance of β-cell mass.

RESULTS

Targeted disruption of the *WFS1* gene

We first studied wfs1 protein expression in the pancreas, as this was essential to understand the diabetic phenotype in mice with a disrupted *wfs1* gene. Mouse pancreas sections were stained using an antibody raised against the 290 amino acid amino-terminus peptide of murine WFS1 (α-mWFS1-N) and those against islet hormones (Fig. 1A–L). Importantly, the WFS1 protein is strongly expressed in β-cells, and the majority of α, δ and F-cells are essentially devoid of wfs1 protein immunoreactivity. Double-staining of dispersed islet cells with these antibodies showed >80% of insulin-positive cells to be stained with anti-WFS1 antibody, while few cells express both WFS1 protein and one of the following: glucagon, somatostatin or pancreatic polypeptide (Fig. 1M–P).

In order to study the pathophysiology of Wolfram syndrome, we sought to inactivate the *wfs1* gene by inserting a neomycin-resistance gene into the second exon of the *wfs1* gene which contains the initial ATG codon (Fig. 2A and B). When analyzed using an antibody against α-mWFS1-N, WFS1 protein bands of 95 kDa were abolished in whole-brain lysates from mutant mice (Fig. 2C). In addition, WFS1 protein staining was detected in neither pancreatic islets (Fig. 2D and E) nor the hippocampus (Fig. 2F and G) in mutant animals. It was subsequently recognized that our disruption strategy resulted in altered splicing transcripts in mutant animals. Reverse transcription–polymerase chain reaction on brain, heart and islet mRNA revealed existence of a *wfs1* mRNA that lacks exon 2 in mutant animals (data not shown). Such an altered mRNA was not detected in wild-type tissues. The mutant transcript could generate amino-terminus-truncated WFS1 protein resulting from initiation of translation from one of the internal methionines. There exist methionine residues at 81, 184, 230 and 299, as well as further downstream, in murine WFS1 protein. We constructed a cDNA encoding WFS1 protein lacking the first 80 amino acids (WFS1-del80) and expressed it in COS7 cells. The WFS1-del80 protein was recognized by the antibody α-mWFS1-N (data not shown), while no bands were detected in brain lysates from mutant animals (Fig. 2C), indicating that WFS1-del80 is not expressed in mutant mice and that mutant proteins, if present, would be WFS1 protein lacking the first 183 amino acids or with larger truncations. We speculate that such truncated WFS1 proteins do not have normal functions since human substitution mutations at alanine 126, alanine 133 or glutamate 169 and a deletion mutation that lacks both lysine 178 and alanine 179 residues cause Wolfram syndrome (5). Therefore, we conclude that WFS1 function is lost, or at least severely impaired, in mice with a disrupted *wfs1* gene.

Mice homozygous for the mutated *wfs1* gene constitute the expected 25% of offspring born to heterozygous mutant parents, and are normal in appearance, growth and fertility. We did not see ataxic posture or gait disturbance. In addition, there were no differences in urine osmolality between wild-type and mutant mice. In the following experiments only male mice were used because an earlier study indicated females to have a milder phenotype. Since juvenile-onset diabetes mellitus is the most prominent feature of Wolfram syndrome, we have focused on this issue herein. Detailed studies on other aspects of this syndrome, including optic atrophy, hearing disorders, diabetes insipidus or psychiatric illness, are currently underway.

Impaired glucose homeostasis in mutant mice

Blood glucose levels in these mice were studied in non-fasted states. Initially, using mice on the [(129Sv × B6) × B6]F2 hybrid background, we found that blood glucose levels of mutant mice started to rise at around 16 weeks of age and >60% of mice (8 out of 13) had overt diabetes by 36 weeks (Fig. 3A). Since the heterogeneous contribution of B6 and 129Sv strains in the mixed background mice could cause a large variance in data, making interpretation difficult, we sought to generate mutant animals on a nearly homogenous genetic background. For this purpose, male mice with a disrupted *wfs1* gene were backcrossed for five successive generations with female mice of the B6 strain, which is frequently used for diabetes and obesity research. On the B6 background, no apparent increase in blood glucose levels was observed even at 36 weeks in mice homozygous for disrupted *wfs1* alleles (Fig. 3B). However, impaired glucose homeostasis was evident in mice on the B6 background when they were subjected to oral glucose tolerance test (Fig. 3C). Blood glucose levels at 15 and 30 min were significantly higher in mutant than in wild-type mice at 17 weeks of

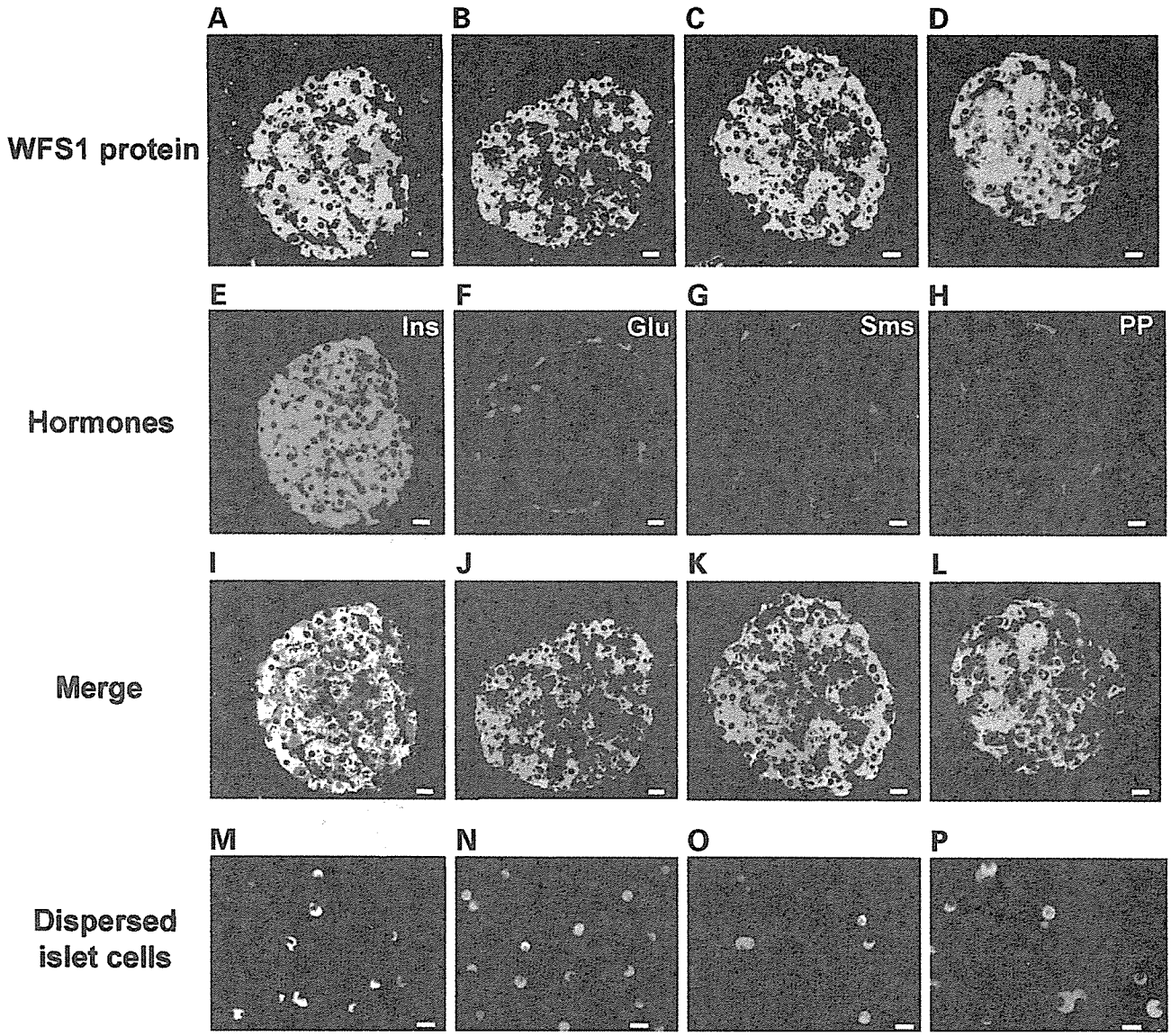

Figure 1. β-Cell specific expression of WFS1 protein in the pancreas. (**A–L**) Paraffin embedded mouse pancreatic sections were immunostained with antibodies against WFS1 protein (green) (A–D) and islet hormones (red): insulin (E), glucagon (F), somatostatin (G), or pancreatic polypeptide (H). A and E are the same section, and the two are merged in I. Similarly, J, K, L are merged versions of B and F, C and G, D and H, respectively. Bars = 10 μm. Ins, insulin; Glu, glucagon; Sms, somatostatin; PP, pancreatic polypeptide. (**M–P**) Dispersed islet cells were stained with anti-WFS1 antibody (green) together with those against islet hormones (red): insulin (M), glucagon (N), somatostatin (O) or pancreatic polypeptide (P). Bars = 10 μm.

age. These data indicated that disruption of the *wfs1* locus induced impaired glucose homeostasis in mice, as is seen in human Wolfram syndrome.

In order to investigate the pathophysiology of impaired glucose homeostasis in mutant mice, plasma immunoreactive insulin (IRI) levels in response to a glucose load were evaluated. Although plasma insulin levels after a 6 h fast were comparable between wild-type and mutant animals at 17 weeks of age (Fig. 3D), hormone responses were markedly blunted in WFS1-deficient mice. We also studied non-fasting plasma insulin levels in these mice. Plasma insulin levels in mutant mice were similar to that in wild-type mice at 24 weeks but had decreased to half the wild-type level at 36 weeks (Fig. 3E). Intraperitoneal insulin injection tests did not show insulin resistance in mutant mice at 14 (data not shown) and 19 weeks (Fig. 3F). In fact, WFS1-deficient mice were somewhat more insulin sensitive. Taken together, these data indicate impaired glucose homeostasis in mice with a disrupted *wfs1* gene to be due to insulin secretory defects rather than insulin resistance.

Impaired stimulus–secretion coupling in β-cells from mutant mice

Since defects in both stimulus–secretion coupling and insulin production could be the cause of insulin secretory defects *in vivo*, insulin secretory responses were studied using isolated islets. When we isolated islets from these mice, we noticed that

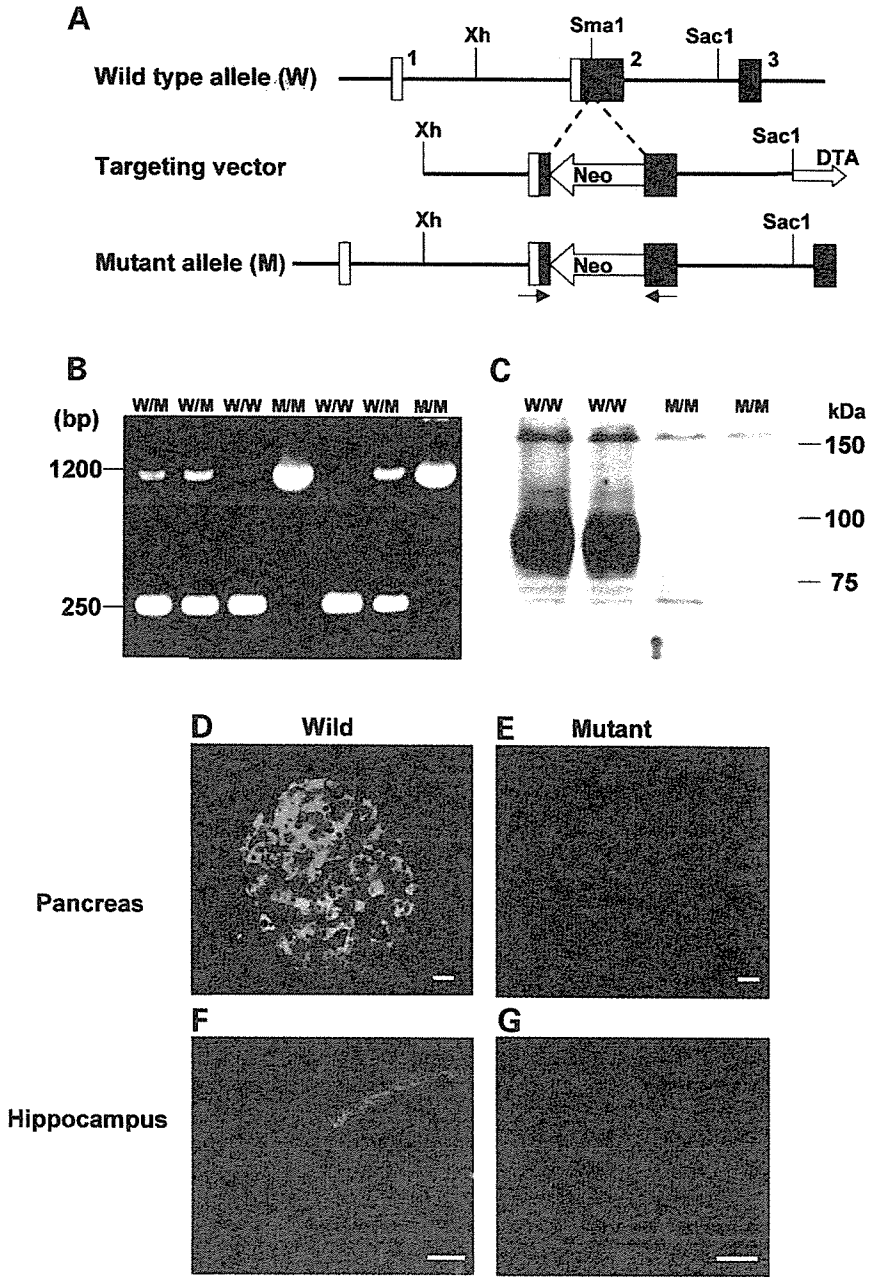

Figure 2. Targeted disruption of the *WFS1* gene. (**A**) Schematic representation of the mouse *wfs1* targeting strategy. Boxes are exons. Neo, neomycin resistance gene; DTA, diphtheria toxin A chain gene. (**B**) PCR genotyping of mutant mice. A 1200 bp longer band is observed in DNA from the disrupted allele. (**C**) Western blot analysis using whole-brain lysates from wild-type and mutant animals probed with anti-WFS1 antibody. (**D–G**) Immunohistochemical analyses using anti-WFS1 antibody in pancreatic (D, E) and hippocampal (F, G) tissues from 14-week-old wild-type and mutant mice. Bars = 10 μm for pancreatic sections and 50 μm for hippocampal sections.

it was possible to obtain only 100 islets or even less from a mutant mouse, while around 200 islets can normally be isolated from a wild-type mouse. Insulin content in the WFS1-deficient islets was slightly (16%) but significantly less than that in islets of wild-type mice [61.8 ± 2.3 ng/islet ($n = 10$ experiments) versus 73.4 ± 3.3 ($n = 10$ experiments), $P = 0.039$, mutant and wild-type islets, respectively]. We used these islets infected with either AdCAGlacZ (as a control) or AdCAGmWFS1 (Fig. 4A), because we also wanted to examine effects of WFS1 re-expression in WFS1-deficient islets and of its overexpression in wild-type islets. Glucose (15 mM)-stimulated insulin secretion, after normalization with insulin content, was reduced by 23% in islets from mutant mice (Fig. 4B). Carbachol (1.0 mM)-stimulated insulin secretion, which is thought to be evoked by Ca^{2+} release from the ER and Ca^{2+} entry through the Ca^{2+} release-activated channel, was also reduced by 26% (Fig. 4C). When WFS1 protein was re-expressed in islets from mutant animals via a recombinant adenovirus,

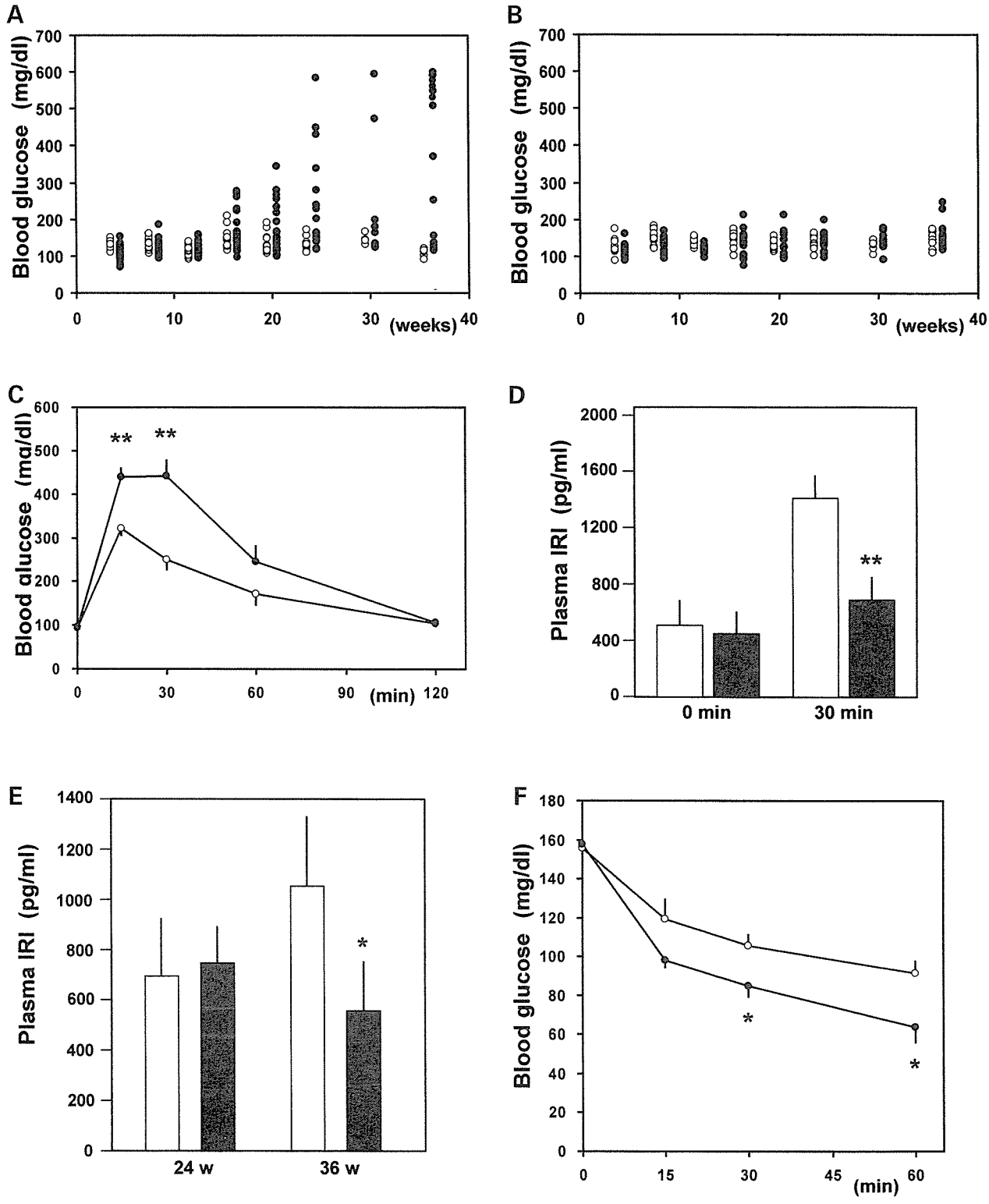

Figure 3. Impaired glucose homeostasis in WFS1-deficient mice. (**A**) Non-fasted blood glucose levels in male mice on the [(129Sv × B6) × B6]F2 hybrid background at indicated ages ($n = 8–13$). (**B**) Non-fasted blood glucose levels in male mice on the B6 background ($n = 9–16$). (**C, D**) Oral glucose (2 mg/g body weight) tolerance test in 17-week-old mice on the B6 background ($n = 6$). Blood glucose levels (C) at indicated points and plasma IRI levels (D) before and 30 min after the glucose load are shown. Glucose tolerance tests were performed on two other occasions using different animals with essentially same results. (**E**) Plasma IRI levels at 24 and 36 weeks of age ($n = 6–8$). (**F**) Insulin (0.75 units/kg body weight) tolerance test at 19 weeks ($n = 5$). Insulin tolerance tests were performed on two other occasions with essentially same results. White circles and bars, wild-type mice; black circles and bars, mutant mice. $^{*}P < 0.05$, $^{**}P < 0.01$.

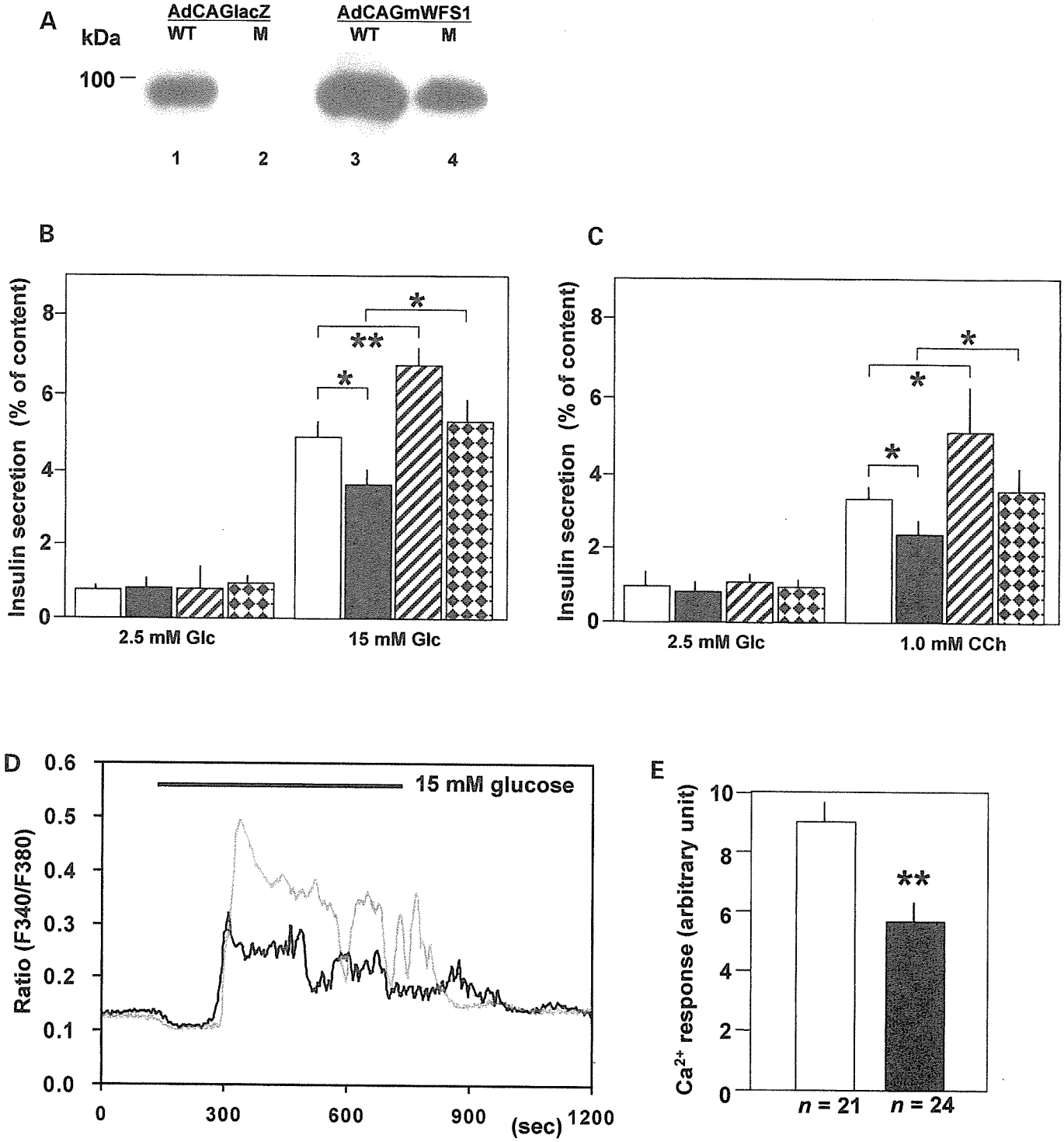

Figure 4. Impaired stimulus–secretion coupling in WFS1-deficient β-cells. (**A**) Islets from wild-type and mutant mice were infected with either AdCAGlacZ or AdCAGmWFS1. After 36 h, islets were subjected to western blot analyses using anti-WFS1 antibody. Lane 1, wild-type islets infected with AdCAGlacZ; lane 2, mutant islets infected with AdCAGlacZ; lane 3, wild-type islets infected with AdCAGmWFS1; lane 4, mutant islets infected with AdCAGmWFS1. Western blot experiments were performed twice with similar results and one of them is shown. (**B**, **C**) Islets were challenged with 15 mM glucose (B) or 1 mM carbachol in the presence of 2.5 mM glucose (C) for 1 h. Absolute insulin secretion in response to glucose was 3.11 ± 0.34 and 2.03 ± 0.26 ng/islet/h, respectively, for wild-type and mutant islets infected with the control virus (AdCAGlacZ). Data are means ± SEM, $n = 5$ experiments. White bars, wild-type islets infected with AdCAlacZ; black bars, mutant islets with AdCAGlacZ; hatched bars, wild-type islets with AdCAGmWFS1; dotted bars, mutant islets with AdCAGmWFS1. (**D**, **E**) Intracellular Ca^{2+} responses to 15 mM glucose in wild-type (gray line and white bar) and WFS1-deficient (black line and black bar) β-cells. Representative traces out of 21 wild-type and 24 WFS1-deficient β-cells from one experiment were shown in D. Areas under the curve during a 5 min period after the onset of Ca^{2+} rises to glucose were summarized in E. Similar significant differences were observed in the other four experiments. $^{*}P < 0.05$, $^{**}P < 0.01$.